after labeling with a combination of PE-anti-CD8 and anti-PE microbeads. The purity was over 95% as determined by using a flow cytometer (Becton Dickinson, Mountain View, CA). For APCs, T cell-depleted spleen cells and EL-4 cells were used after irradiation (30 Gy) and cultured in RPMI1640 medium supplemented with 10% FBS and antibiotics (complete medium).

2.7. CTL assay

The activity of cytotoxic T cells was estimated by measuring the amount of fragmented DNA in target cells using the JAM test [21]. For target cells, Renca tumor cells (H-2^d), stably transfected with SAG1, were labeled overnight with 2 μCi/ml of ^{3}H-thymidine. The target cells were collected, washed, and resuspended at a concentration of 2×10^5 cells/ml in complete medium. Then, 100 μl of this solution was added to each well of a 96-well U-bottom plate. For effecter cells, $CD8^+$ T cells isolated from BALB/c mice (H-2^d) 2 weeks after immunization were stimulated with irradiated target cells for 5 days in vitro and were then collected, washed, and resuspended in complete medium at 5×10^6 cells/ml. The effecter cell suspension (100 μl) was added to each well of the 96-well U-bottom plate at various effecter:target cell ratios. The plate was centrifuged for 5 min at 2000 × *g* and then incubated for 4.5 h at 37 °C in 5% CO_2. After incubation, the plate was harvested onto a glass fiber filter (Packard Instrument B.V. Chemical Operations, Groningen, The Netherlands) using a 96-well harvester (Packard), and the radioactivity trapped on the filter was measured with a beta counter (Packard). The percent DNA fragmentation was calculated using the following formula: (spontaneous counts − experimental counts)/spontaneous counts × 100.

2.8. Quantitative real-time PCR

Quantification of mRNA of IFN-γ or perforin was performed with a real-time PCR system (Applied Biosystems, Foster City, CA), using SYBR Green I double-strand DNA binding dye. Total RNA extracted from splenic $CD8^+$ T cells infected with *T. gondii* was reverse-transcribed followed by PCR. For perforin, the sense and antisense primers were 5′-GATGTGAACCCTAGGCCAGA-3′ and 5′-GGTTTTTGTAC CAGGCGAAA-3′, respectively. For IFN-γ, the sense and antisense primers were 5′- AGCGGCTGACTGAACTCAGA TTGTAG-3′ and 5′-GTCACAGTTTTCAGCTGTATAGGG-3′, respectively. Fluorescence data collected after each extension step were analyzed using software (Applied Biosystems). The relative ratio of mRNA of IFN-γ in each sample was normalized to the relative quantity of β-actin.

2.9. IFN-γ measurement

$CD8^+$ T cells (2.5×10^5) isolated from vaccinated mice were cultured with irradiated T cell-depleted spleen cells (1×10^5) from various mice infected with *T. gondii* or irradiated EL-4 cells transfected with pcDNA-SAG1 or pcDNAUB-SAG1. After 72 h, supernatants were collected, and the cytokine concentration was determined by sandwich ELISA following the instructions of the manufacturer (R&D Systems).

3. Results

3.1. Construction of a chimeric DNA encoding ubiquitin-fused SAG1

We constructed two plasmid vectors encoding truncated SAG1 (the signal sequence was removed) (Fig. 1A). One solely consisted of truncated SAG1, pcDNA-SAG1; the other, designated pcDNAUB-SAG1, was a chimeric DNA encoding a fusion protein (predicted to be processed by the ubiquitin–proteasome system) linking murine ubiquitin (UB) to the N-terminus of SAG1. These two vectors were transfected into COS-7 cells and their expression was confirmed.

3.2. Detection of SAG1 mRNA in the draining lymph nodes of mice vaccinated with pcDNA-SAG1

We reported previously that genes delivered to the skin by gene gun technology are expressed in dendritic cells (DCs) and those cells migrate to the draining lymph nodes [22]. In the current study, the expression of SAG1 mRNA derived from pcDNA-SAG1 was confirmed by RT-PCR using axillary and inguinal lymph node cells 48 h after delivery of the SAG1 gene via skin using the gene gun (Fig. 1B). This finding supports, again, that migratory cells, probably DCs, located in subcutaneous tissue migrate into draining lymph nodes after being inoculated with naked DNA. Furthermore, the expression of SAG1 mRNA was also observed in the gene-transfected skin tissue (data not shown).

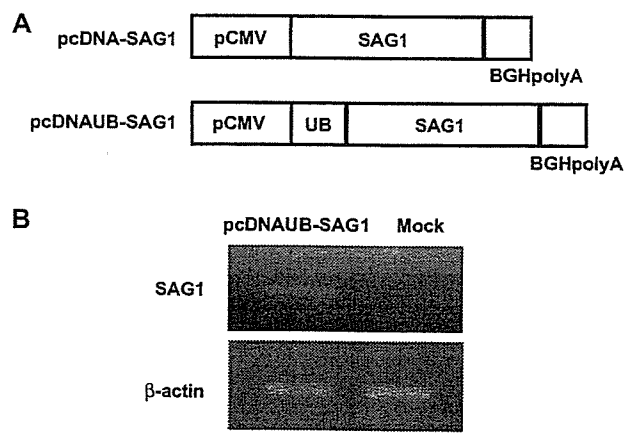

Fig. 1. Generation of pcDNA-SAG1 and pcDNAUB-SAG1 and detection of SAG1 mRNA. (A) Schematic representation of the two plasmids used in this study. The basic form, pcDNA-SAG1, encodes unmodified SAG1. The ubiquitin-fusion form, pcDNAUB-SAG1, encodes chimeric ubiquitin–SAG1 protein. (B) Detection of SAG1 mRNA in draining lymph nodes by RT-PCR. Total RNA samples were prepared from the draining axially and inguinal lymph node cells of mice 48 h after immunization with pcDNA-SAG1 or mock pcDNA.

3.3. Ubiquitin–SAG1 fusion protein is degraded by the proteasome

COS-7 cells were transfected with pcDNA-SAG1 or pcDNAUB-SAG1 and were cultured for 24 h with a proteasome-specific inhibitor, epoxomicin. Harvested cells were lysed, separated by SDS-PAGE and subjected to immunoblotting with anti-SAG1 antibody to determine the level of protein expression (Fig. 2A, B). SAG1 was strongly expressed in COS-7 cells transfected with pcDNA-SAG1 and its expression level was not affected by the inclusion of a proteasome inhibitor, epoxomicin. In contrast, SAG1 was only weakly expressed in cells transfected with pcDNAUB-SAG1, while its expression level was markedly enhanced in the presence of epoxomicin. These results strongly suggest that SAG1 is synthesized in the cytosol of COS-7 cells transfected with pcDNAUB-SAG1 but promptly degraded by the proteasome, whereas the protein accumulates when proteasome activity has been blocked by epoxomicin. Thus, ubiquitin fused with SAG1 must play a key role in the processing of SAG1 by the proteasome.

3.4. Vaccination with pcDNAUB-SAG1 develops potent protective immunity against infection with the highly virulent T. gondii, but not with pcDNA-SAG1

BALB/c mice were vaccinated via the abdominal skin with pcDNA (empty vector), pcDNA-SAG1 and pcDNAUB-SAG1 by using a gene gun, and protective immunity against infection with the highly virulent RH strain was evaluated by their survival rate. Mice were vaccinated four times at 2-week intervals. Two weeks after the final DNA vaccination, mice were challenged intraperitoneally with a lethal dose of 70 tachyzoites of *T. gondii* (Fig. 3A). All groups of mice vaccinated with either pcDNA or pcDNA-SAG1 died within 10 days. In contrast, potent protective immunity was induced in mice vaccinated with pcDNAUB-SAG1. Six of the seven mice in this group survived the challenge. This result suggested that targeting of antigen SAG1 for degradation through the UPS results in a remarkable induction of the protective immune response.

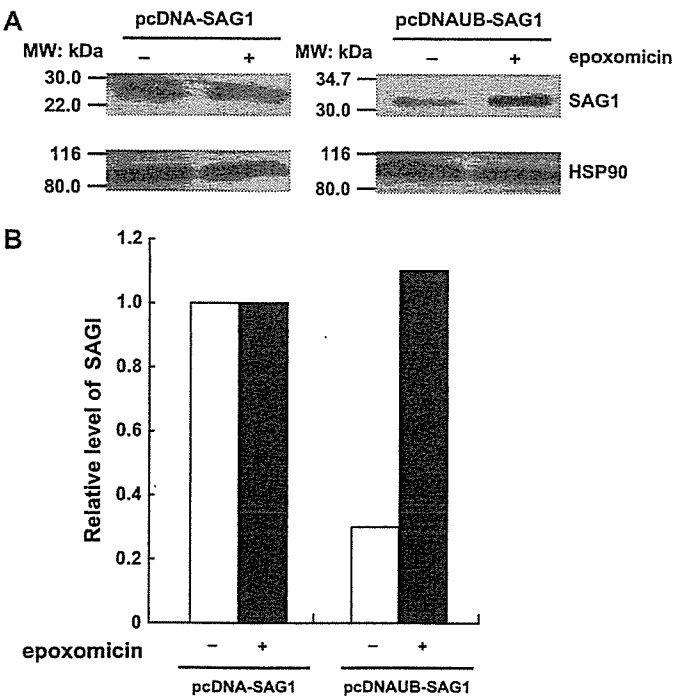

Fig. 2. Proteasomal degradation of ubiquitin–SAG1 fusion protein. (A) COS-7 cells transfected with the indicated plasmid were cultured for 24 h in the presence or absence of epoxomicin. The protein extracts were immunoblotted with antiserum to SAG1. Levels of hsp90 were also examined as an internal control. (B) The expression of SAG1 was densitometrically quantified. Results represent the relative ratio of the level of SAG1 in pcDNA-SAG1-transfected COS-7 cells in the absence of epoxomicin after normalization with hsp90 expression.

3.5. Optimal activation of CTL requires accelerated degradation of ubiquitin-fusion SAG1 by proteasomes

To prove our working hypothesis that ubiquitin-fusion antigens activate $CD8^+$ T cells via the proteasome pathway, we examined, in vitro, whether SAG1, which is essentially an exogenous antigen, is processed by the cytosolic proteasome if it is artificially fused with ubiquitin and expressed in the cytosol. Then we examined the functional properties of $CD8^+$ T cells in mice vaccinated with pcDNAUB-SAG1. $CD8^+$ T cell-dependent protective immune responses have been shown to correlate well with cytolytic behavior and perforin/interferon γ (IFN-γ) production [23]. $CD8^+$ spleen cells from mice inoculated with pcDNAUB-SAG1 were assayed for their cytolytic activity against syngeneic BALB/c-derived Renca tumor cells stably transfected with SAG1. These $CD8^+$ T cells demonstrated a high degree of CTL activity against SAG1-expressing tumor cells (Fig. 3B) but not against parental cells (data not shown), indicating successful induction of antigen-specific $CD8^+$ T cells. Furthermore, they contained large amounts of mRNA encoding perforin, one of the crucial molecules for exerting CTL activity (Fig. 3C). We also assayed IFN-γ production in $CD8^+$ T cells. Real-time PCR quantification of mRNA isolated from $CD8^+$ spleen cells demonstrated a marked increase in message levels upon vaccination of mice with pcDNAUB-SAG1 (Fig. 3D). In addition, IFN-γ was secreted in large amounts in culture supernatants of $CD8^+$ T cells purified from mice vaccinated with pcDNAUB-SAG1 after stimulation with APC from infected mice (Fig. 3E). There was no evidence of activation of $CD8^+$ T cells in mice vaccinated with pcDNA-SAG1 (Fig. 3B–E).

3.6. APCs transfected with pcDNAUB-SAG1 were superior to those with pcDNA-SAG1 in activating $CD8^+$ T cells but activity was eliminated by the proteasome inhibitor epoxomicin

To confirm that the potent $CD8^+$ T cell responses were induced by the product of ubiquitin-directed proteasome degradation, we examined the effect of epoxomicin on antigen presentation to $CD8^+$ T cells of C57BL/6 (B6) mice vaccinated with pcDNAUB-SAG1. Transfected EL-4 cells were incubated with or without epoxomicin for 24 h. After extensive

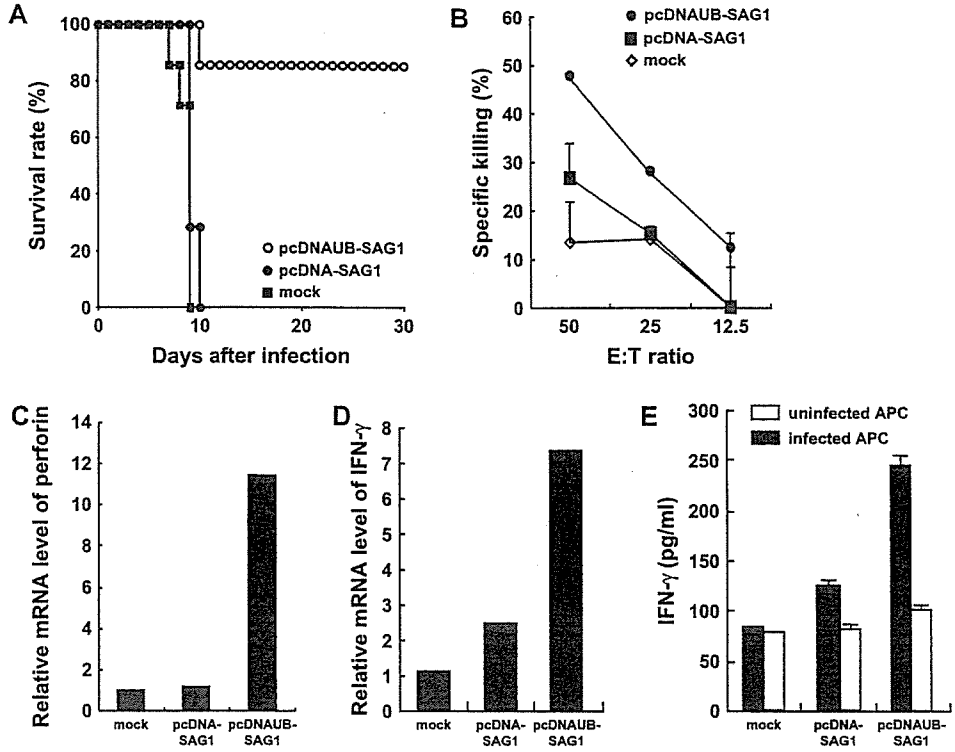

Fig. 3. Protective immunity against a highly virulent strain of *T. gondii* in mice vaccinated with pcDNAUB-SAG1 and the crucial role of the proteasome in induction of $CD8^+$ T cell-mediated immunity. (A) BALB/c mice were vaccinated with SAG1 vectors by the use of a gene gun four times at 2-week intervals. Two weeks after the final vaccination, mice ($n=7$) were infected with a lethal dose of 70 tachyzoites of *T. gondii*. The survival rate of mice vaccinated with the indicated vectors was monitored. (B) The CTL activity was estimated by measuring the amount of fragmented DNA in target cells using the JAM test. Splenic $CD8^+$ T cells purified from mice vaccinated with the indicated vector were added to target cells at the indicated ratio after stimulation with irradiated target cells for 5 days. After 4.5 h of incubation, radioactivity was counted with a β counter. (C, D) Total RNA extracted from splenic $CD8^+$ T cells purified from mice vaccinated with the indicated plasmids and infected with *T. gondii* were reverse-transcribed followed by PCR. Quantification of mRNA of perforin and IFN-γ was performed using real-time PCR. The relative ratio of the signals in each sample was normalized to the relative quantity of β-actin. The experiment was repeated three times, and similar results were obtained. (E) $CD8^+$ T cells purified from the spleen of mice 2 weeks after the final vaccination were cultured with irradiated T cell-depleted splenocytes as APC prepared from infected or uninfected BALB/c mice. Culture supernatants were harvested 72 h later, and IFN-γ concentration was determined by sandwich ELISA.

washes to remove epoxomicin, SAG1-expressing EL-4 cells were co-cultured with purified $CD8^+$ T cells from vaccinated mice. Then, IFN-γ concentrations in these culture supernatants were assayed by sandwich ELISA (Fig. 4). Production was markedly greater in the group of APCs transfected with pcDNAUB-SAG1 than in the APCs transfected with pcDNA-SAG1. Thus, EL-4 cells transfected with pcDNAUB-SAG1 were superior to cells containing pcDNA-SAG1 in inducing the cytokine production by specific $CD8^+$ T cells, indicating that ubiquitin–SAG1 protein was efficiently processed and presented to MHC class I molecules via the UPS in pcDNAUB-SAG1 group. The production of IFN-γ in both groups of APCs was almost completely abolished when epoxomicin was added to the culture, suggesting again that the proteasome/UPS in APC plays a crucial role in the activation of SAG1-specific $CD8^+$ T cells producing IFN-γ.

3.7. Protection by UB–SAG1 vaccine is impaired in LMP7-deficient mice

LMP7 is an immuno-subunit of the 20S core proteasome [14]. We employed LMP7-deficient mice to confirm the contribution of immunoproteasomes to protective immunity. B6.LMP7-deficient mice were vaccinated with pcDNAUB-SAG1 and challenged with the RH strain of *T. gondii*. As shown in Fig. 5A, the infection was controlled in four of the six B6 mice vaccinated with pcDNAUB-SAG1, although B6 mice are generally regarded as highly susceptible to *T. gondii* infection compared with BALB/c mice. In contrast, only two of the six LMP7-deficient mice survived, indicating that vaccination with pcDNAUB-SAG1 is ineffective in LMP7-deficient mice.

To evaluate the activity of $CD8^+$ T cells in wild-type and LMP7-deficient mice, splenic $CD8^+$ T cells purified from mice vaccinated with pcDNAUB–SAG1 were cultured with APCs prepared from wild-type B6 mice infected with *T. gondii*, and culture supernatants were collected and tested for IFN-γ by ELISA (Fig. 5B). $CD8^+$ T cells from B6.LMP7-deficient mice failed to produce IFN-γ in response to APCs from infected wild-type mice, the APCs of which were capable of activating $CD8^+$ T cells from wild-type mice vaccinated with pcDNAUB-SAG1. It should be noted that $CD4^+$ T cells from the deficient mice were immunocompetent since those cells could generate IFN-γ at the same level as that generated

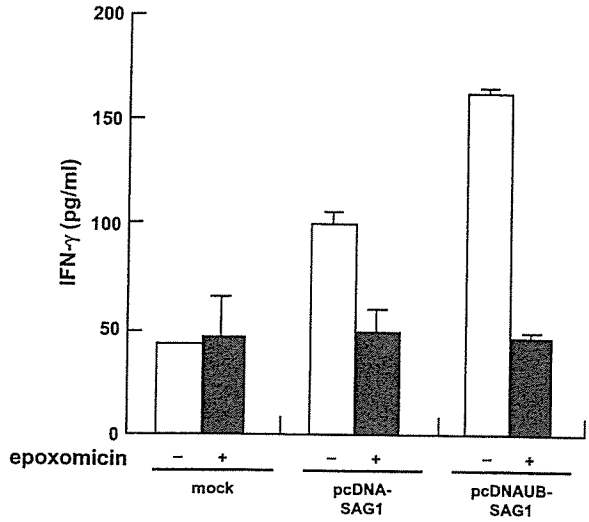

Fig. 4. Function of APCs transfected with pcDNAUB-SAG1 or pcDNA-SAG1 and proteasome-dependent activation of $CD8^+$ T cells. $CD8^+$ T cells purified from a B6 mouse vaccinated with pcDNA-SAG1 or pcDNAUB-SAG1 were co-cultured with irradiated syngeneic EL-4 cells transfected with the indicated vectors in the presence or absence of epoxomicin for 72 h. The culture supernatants were analyzed for IFN-γ concentration.

by cells from wild-type B6 mice when those mice had been vaccinated with either pcDNAUB-SAG1 or pcDNA-SAG1 (data not shown). Thus, protective immunity conferred by vaccination with pcDNAUB-SAG1 was mediated mainly by $CD8^+$ T cells that developed in an LMP7-dependent manner.

3.8. PA28 is not required for induction of CTL by vaccination with pcDNAUB-SAG1

The PA28α/β complex is a proteasome regulator ordinarily associated with the 20S core immunoproteasome [24]. We reported previously that the PA28α/β complex plays an essential role in the processing of a murine melanoma antigen, tyrosinase-related protein (TRP-2), and in the activation of specific $CD8^+$ CTL via the UPS [15]. We therefore examined whether the PA28α/β complex contributes to the protective immunity described here. B6.PA28α/β-deficient mice were vaccinated with pcDNAUB-SAG1 and challenged with the RH strain of *T. gondii*. Four of six PA28α/β-heterozygous mice and three of six PA28α/β-deficient mice survived the challenge, indicating that vaccination with pcDNAUB-SAG1 is efficacious even in PA28α/β-deficient mice (Fig. 6A). $CD8^+$ T cells from PA28α/β-deficient mice could produce IFN-γ at the same level as that produced by $CD8^+$ T cells from PA28α/β-heterozygous mice, which correlated with the grade of protective immunity (Fig. 6B). Thus, protective immunity acquired by vaccination with pcDNAUB-SAG1 developed in a PA28α/β-independent manner.

3.9. The potential of APCs from LMP7$^{-/-}$ or PA28α/β$^{-/-}$ mice to activate $CD8^+$ T cells is different

Potent activation of $CD8^+$ T cells in wild-type mice vaccinated with pcDNAUB-SAG1 appears to be dependent on accelerated processing of SAG1 in their APC. To further confirm the role of the UPS in effective vaccination in the present system, $CD8^+$ T cells from pcDNAUB-SAG1-vaccinated mice were stimulated with APCs from *T. gondii*-infected wild-type mice and two mutant strains of mice mentioned above, and then levels of IFN-γ production in the groups were compared (Fig. 7). APCs from wild-type (WT) B6 mice could activate $CD8^+$ T cells from the vaccinated mice, resulting in secretion of a large amount of IFN-γ. APCs from LMP7-deficient mice failed to induce cytokine production by the responsible $CD8^+$ T cells. On the other hand, APCs from PA28α/β-deficient mice could support IFN-γ production by $CD8^+$ T cells as well as those from wild-type mice. Thus, it was confirmed that LMP7 is essential for the effective processing of SAG1 but PA28α/β is not. It should be noted that the mutant mice used in this study showed no alteration in ratios of $CD4^+$ and $CD8^+$ T cells to whole spleen or lymph node cells (data not shown).

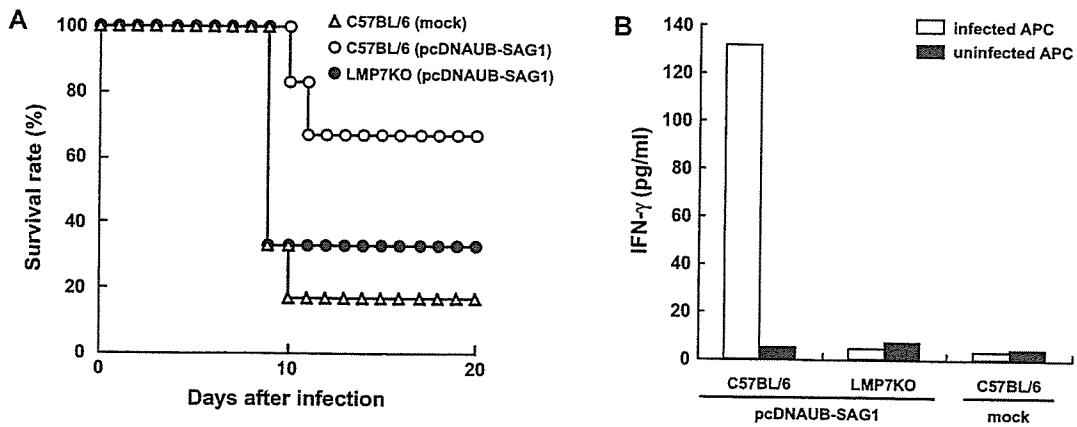

Fig. 5. Susceptibility and impaired $CD8^+$ T cell activation in B6.LMP7-deficient mice vaccinated with pcDNAUB-SAG1. (A) B6.LMP7-deficient ($n = 6$) and wild-type mice ($n = 6$) vaccinated with the indicated vector were infected with *T. gondii*, and the survival rate was monitored. (B) Splenic $CD8^+$ T cells purified from mice vaccinated with pcDNAUB-SAG1 were cultured with irradiated APCs prepared from infected or uninfected wild-type mice, and culture supernatants were tested for IFN-γ.

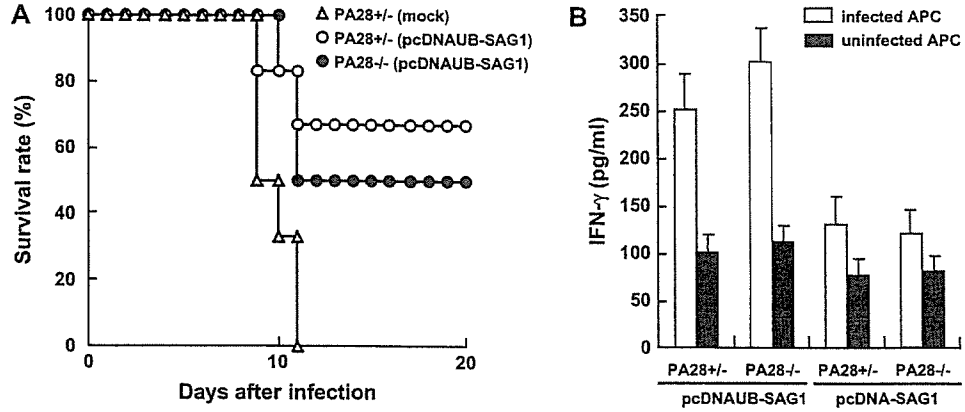

Fig. 6. PA28-independent protection and activation of $CD8^+$ T cells. (A) B6.PA28$\alpha/\beta^{-/-}$ ($n=6$) or PA28$\alpha/\beta^{+/-}$ mice ($n=6$) were vaccinated with pcDNAUB-SAG1, and PA28$\alpha/\beta^{+/-}$ mice were vaccinated with pcDNA four times at 2-week intervals. Two weeks after the final vaccination, mice ($n=7$) were infected with a lethal dose of 70 tachyzoites of *T. gondii*. (B) Splenic $CD8^+$ T cells purified from PA28$\alpha/\beta^{-/-}$ or PA28$\alpha/\beta^{+/-}$ mice vaccinated with pcDNA-SAG1 or pcDNAUB-SAG1 were cultured with irradiated APCs from *T. gondii*-infected or uninfected B6 mice.

4. Discussion

In the present study, we developed a new DNA vaccination strategy against infection with the highly virulent RH strain of *T. gondii* by constructing a chimeric gene encoding a fusion protein between murine ubiquitin and full-length SAG1. Vaccination with the chimeric DNA induced antigen-specific CTL activity and conferred potent protection to infection with the highly virulent RH strain of *T. gondii*.

$CD8^+$ T cells and IFN-γ have been shown to play crucial roles in protective immunity against *T. gondii* in either acute or chronic infection [25–30]. Our preliminary experiment showed that vaccination of DNA encoding only SAG1, cannot induce protection in mice infected with the highly virulent RH strain of *T. gondii*. Therefore, we constructed the vaccine vector encoding ubiquitin-fused SAG1 which was expected to be processed by the UPS and then expressed on the surface of MHC class I molecules, resulting in the activation of SAG1-specific $CD8^+$ T cells. Involvement of the UPS in antigen processing was first suggested by Townsend et al. They observed that enhanced degradation of a viral protein fused with the ubiquitin moiety facilitates the formation of CTL epitopes [31]. Subsequently, enhanced CTL response was also observed when the amino terminal residues of β-galactosidase [32] or HIV-1 envelop protein [33] were modified according to the N-end rule [34] so as to make those proteins more susceptible to ubiquitin-dependent cytoplasmic degradation. Immunoblotting experiments shown in Fig. 2A, B indicate that the SAG1 protein fused with ubiquitin is highly efficiently degraded in COS-7 cells compared with unmodified SAG1 protein, and that degradation of the fusion protein is inhibited by a proteasome inhibitor, epoxomicin. Based on the in vitro experiment mentioned above, we developed a new DNA vaccine strategy against the highly virulent *T. gondii*. Vaccination with the chimeric DNA exerted excellent protective immunity against the infection via activation of SAG1-specific $CD8^+$ T cells/CTLs. These SAG1-specific $CD8^+$ T cells had the capability of producing perforin and IFN-γ to kill infected target cells which should be important in protecting against the high virulent *T. gondii*. Furthermore, activation of these T cells was blocked by epoxomicin as shown in Fig. 4.

The immunomodulatory cytokine IFN-γ, which is produced by activated T helper 1 cells, natural killer (NK) cells and $CD8^+$ T cells, enhances antigen presentation by upregulating MHC and TAP gene products in addition to proteasome subunits and regulators. IFN-γ alters the quality of proteasome activity by incorporating three IFN-γ-induced catalytic subunits, LMP2, LMP7 and MECL-1, to replace the constitutive catalytic subunits (Y/δ, X/MB1 and Z, respectively) in the 20S core proteasome during proteasome biogenesis [14,35,36]. MECL-1 requires LMP2 for efficient incorporation into preproteasomes, and preproteasomes containing LMP2 and MECL-1 require LMP7 for efficient maturation [37]. On these bases, we employed LMP7-deficient mice to confirm the contribution of immunoproteasomes to the protective immunity. The vaccination with pcDNAUB-SAG1 was ineffective in LMP7-deficient B6 mice as shown in Fig. 5A. This

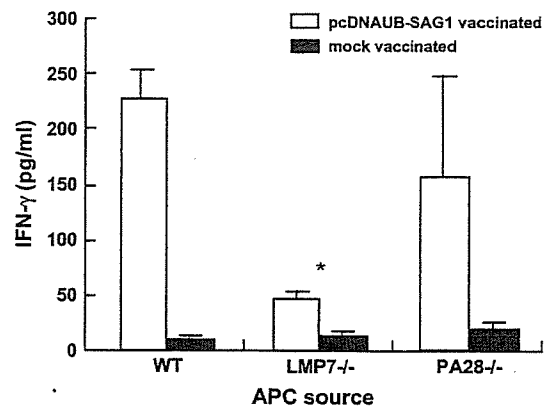

Fig. 7. Function of APCs from LMP7$^{-/-}$ and PA28$\alpha/\beta^{-/-}$ mice. Splenic $CD8^+$ T cells purified from wild-type (WT) B6 mice vaccinated with pcDNAUB-SAG1 were cultured with APCs isolated from wild-type (WT), LMP7$^{-/-}$, or PA28$\alpha/\beta^{-/-}$ mice 4 days after infection with *T. gondii*. Amounts of IFN-γ in the supernatants were assayed by ELISA. Data represent average ± S.D. of three individual mice. The asterisk indicates significance at $P < 0.01$ by Student's *t*-test.

result supports that ubiquitinated SAG1 is processed at least by LMP7 in immunoproteasomes and then is directed to MHC class I molecules, resulting in the activation of SAG1-specific $CD8^+$ T cells in mice vaccinated with pcDNAUB-SAG1.

So far, there are several reports addressing the importance of immunoproteasomes for the production of various MHC class I epitopes, although certain antigenic peptides are known to be generated by standard (or constitutive) proteasomes [38,39]. Immunoproteasomes are functionally different from the standard proteasomes in protease activities and prefer to cleave peptide bonds on carboxyl side of basic and hydrophobic amino acid residues [40–42]. Thus, formation of immunoproteasomes facilitates the production of MHC class I-binding peptides because hydrophobic or basic carboxyl terminal residues normally serve as anchors for binding to MHC class I molecules [43]. Together with the results demonstrating that degradation of SAG1 clearly occurred in COS-7 cells presumably in the absence of immunoproteasomes (Fig. 2), LMP7 is crucial for the generation of class I epitopes but not for the degradation of SAG1. Induction of immunoproteasomes enhances $CD8^+$ T cell activation. Therefore, this might be one of the major targets of IFN-γ secreted by $CD8^+$ T cells, which may form positive feedback loop between APC and $CD8^+$ T cells. It is quite possible that immunoproteasomes are induced in EL-4 cultured with SAG1-specific $CD8^+$ T cells induced in mice vaccinated with pcDNAUB-SAG1 (Figs. 4 and 7).

IFN-γ also regulates the expression of two proteasome regulators PA28α and PA28β, which form the heptameric proteasome activator complex PA28 [24]. This heteromultimer is able to bind to the α rings of the 20S core proteasome, thereby enhancing proteolytic activity, although the mechanism of PA28-mediated enhancement of intrinsic proteasome activity is not fully elucidated [44]. In vitro studies showed that purified PA28α/β can enhance coordinated dual cleavages by the 20S proteasome, leading to augmented epitope liberation [45], and expression of PA28α in mouse fibroblasts increases the sensitivity for lysis by virus-specific CTLs [46]. Furthermore, we found that processing of an epitope derived from the tumor antigen TRP-2 of murine B16 melanoma is entirely dependent on PA28α/β in vitro [15] and in vivo [47,48]. In this study, however, we showed that induction of MHC class I-restricted immunity targeting the *Toxoplasma* SAG1 protein is independent of PA28α/β, although conclusively dependent on the immunoproteasome LMP7. Compensatory systems for PA28α/β function should exist in the UPS [24]. Recently, we found that the processing of antigens is regulated by at least two distinct pathways, that is, the PA28-dependent and hsp90-dependent pathways [49]. These two pathways operate either redundantly or specifically, depending on antigen species and cell types.

Our findings provide evidence for the first time that DNA vaccination with a chimeric gene encoding ubiquitin-fused SAG1 derived from *T. gondii* confers resistance to infection with the highly virulent RH strain of *T. gondii* on host mice through the UFD, in which immunoproteasomes play a critical role independent of the PA28α/β complex. Elucidation of rules for the relationship between the hierarchy of epitopes and the responsible UPS should provide clues for developing effective vaccines against microbes and effective strategies for treating tumors.

Acknowledgements

We thank David G. Russell for his helpful discussion and critical reading of the manuscript. This work was supported by grants-in-aid from the Ministry of Education, Science, Sport, and Culture of Japan (15019075, 15025255, 15390136, 15659265).

References

[1] A. Hershko, A. Ciechanover, The ubiquitin system, Annu. Rev. Biochem. 67 (1998) 425–479.
[2] A.L. Goldberg, K.L. Rock, Proteolysis, proteasomes and antigen presentation, Nature 357 (1992) 375–379.
[3] K. Tanaka, M. Kasahara, The MHC class I ligand-generating system: roles of immunoproteasomes and the interferon-gamma-inducible proteasome activator PA28, Immunol. Rev. 163 (1998) 161–176.
[4] I.A. Khan, K.H. Ely, L.H. Kasper, A purified parasite antigen (p30) mediates CD8+ T cell immunity against fatal *Toxoplasma gondii* infection in mice, J. Immunol. 147 (1991) 3501–3506.
[5] E. Petersen, H.V. Nielsen, L. Christiansen, J. Spenter, Immunization with *E. coli* produced recombinant *T. gondii* SAG1 with alum as adjuvant protect mice against lethal infection with *Toxoplasma gondii*, Vaccine 16 (1998) 1283–1289.
[6] J.L. Burg, D. Perelman, L.H. Kasper, P.L. Ware, J.C. Boothroyd, Molecular analysis of the gene encoding the major surface antigen of *Toxoplasma gondii*, J. Immunol. 141 (1988) 3584–3591.
[7] T. Windeck, U. Gross, *Toxoplasma gondii* strain-specific transcript levels of SAG1 and their association with virulence, Parasitol. Res. 82 (1996) 715–719.
[8] I. Potasman, F.G. Araujo, G. Desmonts, J.S. Remington, Analysis of *Toxoplasma gondii* antigens recognized by human sera obtained before and after acute infection, J. Infect. Dis. 154 (1986) 650–657.
[9] Y. Nakano, H. Hisaeda, T. Sakai, M. Zhang, Y. Maekawa, T. Zhang, M. Nishitani, H. Ishikawa, K. Himeno, Granule-dependent killing of *Toxoplasma gondii* by $CD8^+$ T cells, Immunology 104 (2001) 289–298.
[10] H.V. Nielsen, S.L. Lauemoller, L. Christiansen, S. Buus, A. Fomsgaard, E. Petersen, Complete protection against lethal *Toxoplasma gondii* infection in mice immunized with a plasmid encoding the *SAG1* gene, Infect. Immun. 67 (1999) 6358–6363.
[11] C.W. Angus, D. Klivington-Evans, J.P. Dubey, J.A. Kovacs, Immunization with a DNA plasmid encoding the SAG1 (P30) protein of *Toxoplasma gondii* is immunogenic and protective in rodents, J. Infect. Dis. 181 (2000) 317–324.
[12] A. Fachado, A. Rodriguez, S.O. Angel, D.C. Pinto, I. Vila, A. Acosta, R.R. Amendoria, J. Lannes-Vieira, Protective effect of a naked DNA vaccine cocktail against lethal toxoplasmosis in mice, Vaccine 21 (2003) 1327–1335.
[13] H. Rouard, B. Klonjkowski, J. Marquet, C. Lahet, S. Mercier, M. Andrieu, P. Maison, V. Molinier-Frenkel, M. Eloit, J.P. Farcet, P. Langlade-Demoyen, M.H. Delfau-Larue, Adenoviral transgene ubiquitination enhances mouse immunization and class I presentation by human dendritic cells, Hum. Gene Ther. 14 (2003) 1319–1332.
[14] H.J. Fehling, W. Swat, C. Laplace, R. Kuhn, K. Rajewsky, U. Muller, H. von Boehmer, MHC class I expression in mice lacking the proteasome subunit LMP-7, Science 265 (1994) 1234–1237.
[15] S. Murata, H. Udono, N. Tanahashi, N. Hamada, K. Watanabe, K. Adachi, T. Yamano, K. Yui, N. Kobayashi, M. Kasahara, K. Tanaka, T. Chiba, Immunoproteasome assembly and antigen

presentation in mice lacking both PA28alpha and PA28beta, EMBO J. 20 (2001) 5898–5907.
[16] Y. Ito, Y. Kusunoki, M. Tsuchimoto, M. Doi, M. Furuya, Y. Oka, H. Osaki, Pathogenicity of tachyzoites, cysts and oocysts of *Toxoplasma gondii* Beverley strain in mice, Jpn. J. Parasitol. 25 (1976) 133–140.
[17] A.B. Sabin, Toxoplasmic encephalitis in children, JAMA 116 (1941) 801–807.
[18] H. Nagasawa, M. Oka, K. Maeda, J.-G. Chai, H. Hisaeda, Y. Ito, R.A. Good, K. Himeno, Induction of heat shock protein closely correlates with protection against *Toxoplasma gondii* infection, Proc. Natl. Acad. Sci. U.S.A. 89 (1992) 3155–3158.
[19] H. Hisaeda, H. Nagasawa, K. Maeda, Y. Maekawa, H. Ishikawa, Y. Ito, R.A. Good, K. Himeno, γδ T cells play an important role in hsp65 expression and in acquiring protective immune responses against infection with *Toxoplasma gondii*, J. Immunol 155 (1995) 244–251.
[20] T. Sakai, H. Hisaeda, Y. Nakano, H. Ishikawa, Y. Maekawa, K. Ishii, Y. Nitta, J. Miyazaki, K. Himeno, Gene gun-mediated delivery of an interleukin-12 expression plasmid protects against infections with the intracellular protozoan parasites *Leishmania major* and *Trypanosoma cruzi* in mice, Immunology 99 (2000) 615–624.
[21] P. Matzinger, The JAM test. A simple assay for DNA fragmentation and cell death, J. Immunol. Methods 145 (1991) 185–192.
[22] M.A. Nishitani, T. Sakai, K. Ishii, M. Zhang, Y. Nakano, Y. Nitta, J. Miyazaki, H.O. Kanayama, S. Kagawa, K. Himeno, A convenient cancer vaccine therapy with in vivo transfer of interleukin 12 expression plasmid using gene gun technology after priming with irradiated carcinoma cells, Cancer Gene Ther. 9 (2002) 156–163.
[23] J.T. Harty, A.R. Tvinnereim, D.W. White, $CD8^+$ T cell effector mechanisms in resistance to infection, Annu. Rev. Immunol. 18 (2000) 275–308.
[24] M. Rechsteiner, C. Realini, V. Ustrell, The proteasome activator 11 S REG (PA28) and class I antigen presentation, Biochem. J. 345 (2000) 1–15.
[25] T.M. Scharton-Kersten, T.A. Wynn, E.Y. Denkers, S. Bala, E. Grunvald, S. Hieny, R.T. Gazzinelli, A. Sher, In the absence of endogenous IFN-gamma, mice develop unimpaired IL-12 responses to *Toxoplasma gondii* while failing to control acute infection, J. Immunol. 157 (1996) 4045–4054.
[26] R. Gazzinelli, Y. Xu, S. Hieny, A. Cheever, A. Sher, Simultaneous depletion of $CD4^+$ and $CD8^+$ T lymphocytes is required to reactivate chronic infection with *Toxoplasma gondii*, J. Immunol. 149 (1992) 175–180.
[27] R.T. Gazzinelli, F.T. Hakim, S. Hieny, G.M. Shearer, A. Sher, Synergistic role of $CD4^+$ and $CD8^+$ T lymphocytes in IFN-gamma production and protective immunity induced by an attenuated *Toxoplasma gondii* vaccine, J. Immunol. 146 (1991) 286–292.
[28] Y. Suzuki, J.S. Remington, The effect of anti-IFN-gamma antibody on the protective effect of Lyt-2^+ immune T cells against toxoplasmosis in mice, J. Immunol. 144 (1990) 1954–1956.
[29] Y. Suzuki, M.A. Orellana, R.D. Schreiber, J.S. Remington, Interferon-gamma: the major mediator of resistance against *Toxoplasma gondii*, Science 240 (1988) 516–518.
[30] Y. Suzuki, F.K. Conley, J.S. Remington, Importance of endogenous IFN-gamma for prevention of toxoplasmic encephalitis in mice, J. Immunol. 143 (1989) 2045–2050.
[31] A. Townsend, J. Bastin, K. Gould, G. Brownlee, M. Andrew, B. Coupar, D. Boyle, S. Chan, G. Smith, Defective presentation to class I-restricted cytotoxic T lymphocytes in vaccinia-infected cells is overcome by enhanced degradation of antigen, J. Exp. Med. 168 (1988) 1211–1224.
[32] E.P. Grant, M.T. Michalek, A.L. Goldberg, K.L. Rock, Rate of antigen degradation by the ubiquitin–proteasome pathway influences MHC class I presentation, J. Immunol. 15 (1995) 3750–3758.
[33] T.W. Tobery, R.F. Siliciano, Targeting of HIV-1 antigens for rapid intracellular degradation enhances cytotoxic T lymphocyte (CTL) recognition and the induction of de novo CTL responses in vivo after immunization, J. Exp. Med. 185 (1997) 909–920.
[34] A. Varshavsky, The N-end rule, Cell 29 (1992) 725–735.
[35] K.L. Rock, I.A. York, T. Saric, A.L. Goldberg, Protein degradation and the generation of MHC class I-presented peptides, Adv. Immunol. 80 (2000) 1–70.
[36] P.M. Kloetzel, F. Ossendorp, Proteasome and peptidase function in MHC-class-I-mediated antigen presentation, Curr. Opin. Immunol. 16 (2004) 76–81.
[37] T.A. Griffin, D. Nandi, M. Curz, H.J. Fehling, L.V. Kaer, J.J. Monaco, R.A. Colbert, Immunoproteasome assembly: cooperative incorporation of interferon gamma (IFN-gamma)-inducible subunits, J. Exp. Med. 187 (1998) 97–104.
[38] S. Sijts, D. Zaiss, P.M. Kloetzel, The role of the ubiquitin–proteasome pathway in MHC class I antigen processing: implications for vaccine design, Curr. Mol. Med. 1 (2001) 665–676.
[39] P.M. Kloetzel, Antigen processing by the proteasome, Nat. Rev. Mol. Cell Biol. 2 (2001) 179–187.
[40] M. Aki, N. Shimbara, M. Takashina, K. Akiyama, S. Kagawa, T. Tamura, N. Tanahashi, T. Yoshimura, K. Tanaka, A. Ichihara, Interferon-gamma induces different subunit organizations and functional diversity of proteasomes, J. Biochem. 115 (1994) 257–269.
[41] M. Gaczynska, K.L. Rock, A.L. Goldberg, Gamma-interferon and expression of MHC genes regulate peptide hydrolysis by proteasomes, Nature 365 (1993) 264–267.
[42] J. Driscoll, M.G. Brown, D. Finley, J.J. Monaco, MHC-linked LMP gene products specifically alter peptidase activities of the proteasome, Nature 365 (1993) 262–264.
[43] H.G. Rammensee, T. Friede, S. Stevanoviic, MHC ligands and peptide motifs: first listing, Immunogenetics 41 (1995) 178–228.
[44] O. Coux, K. Tanaka, A.L. Goldberg, Structure and functions of the 20S and 26S proteasomes, Annu. Rev. Biochem. 65 (1996) 801–847.
[45] T.P. Dick, T. Ruppert, M. Groettrup, P.M. Kloetzel, L. Kuehn, U.H. Koszinowski, S. Stevanovic, H. Schild, H.G. Rammensee, Coordinated dual cleavages induced by the proteasome regulator PA28 lead to dominant MHC ligands, Cell 86 (1996) 253–262.
[46] M. Groettrup, A. Soza, M. Eggers, L. Kuehn, T.P. Dick, H. Schild, H.G. Rammensee, U.H. Koszinowski, P.M. Kloetzel, A role for the proteasome regulator PA28α in antigen presentation, Nature 381 (1996) 166–168.
[47] M. Zhang, K. Ishii, H. Hisaeda, S. Murata, T. Chiba, K. Tanaka, Y. Li, C. Obata, M. Furue, K. Himeno, Ubiquitin-fusion degradation pathway plays an indispensable role in naked DNA vaccination with a chimeric gene encoding a syngeneic cytotoxic T lymphocyte epitope of melanocyte and green fluorescent protein, Immunology 112 (2004) 567–574.
[48] M. Zhang, C. Obata, H. Hisaeda, K. Ishii, S. Murata, T. Chiba, K. Tanaka, Y. Li, M. Furue, B. Chou, T. Imai, X. Duan, K. Himeno, A novel DNA vaccine based on ubiquitin–proteasome pathway targeting 'self'-antigens expressed in melanoma/melanocyte, Gene Ther. 12 (2005) 1049–1057.
[49] T. Yamano, S. Murata, N. Shimbara, N. Tanaka, T. Chiba, K. Tanaka, K. Yui, H. Udono, Two distinct pathways mediated by PA28 and hsp90 in major histocompatibility complex class I antigen processing, J. Exp. Med. 196 (2002) 185–196.

INFECTION AND IMMUNITY, Sept. 2006, p. 5292–5301 Vol. 74, No. 9
0019-9567/06/$08.00+0 doi:10.1128/IAI.02024-05

Intestinal Intraepithelial Lymphocytes Sustain the Epithelial Barrier Function against *Eimeria vermiformis* Infection

Kyoko Inagaki-Ohara,[1]* Fitriya Nurannisa Dewi,[2,3] Hajime Hisaeda,[4] Adrian L. Smith,[5] Fumiko Jimi,[2] Maki Miyahira,[2] Ayman Samir Farid Abdel-Aleem,[2] Yoichiro Horii,[2] and Yukifumi Nawa[1]

Parasitic Diseases Unit, Department of Infectious Diseases, Faculty of Medicine, University of Miyazaki, 5200 Kihara, Kiyotake, Miyazaki 889-1692, Japan[1]; Department of Veterinary Teaching Hospital and Internal Medicine, Faculty of Agriculture, University of Miyazaki, Gakuen Kibanadai Nishi, Miyazaki 889-2192, Japan[2]; Faculty of Veterinary Medicine, Bogor Agricultural University, Jalan Agatis Campus IPB Darmaga Bogor 16680, Jawa Barat, Indonesia[3]; Department of Parasitology, Graduate School of Medical Science, Kyushu University, 3-1-1 Higashi-ku, Maidashi, Fukuoka 812-8582, Japan[4]; and Division of Immunology, Institute for Animal Health, Compton, Nr. Newbury, Berkshire RG20 7NN, United Kingdom[5]

Received 16 December 2005/Returned for modification 1 March 2006/Accepted 30 June 2006

***Eimeria* spp. are intracellular protozoa that infect intestinal epithelia of most vertebrates, causing coccidiosis. Intestinal intraepithelial lymphocytes (IEL) that reside at the basolateral site of epithelial cells (EC) have immunoregulatory and immunoprotective roles against *Eimeria* spp. infection. However, it remains unknown how IEL are involved in the regulation of epithelial barrier during *Eimeria* sp. infection. Here, we demonstrated two distinct roles of IEL against infection with *Eimeria vermiformis*, a murine pathogen: production of cytokines to induce protective immunity and expression of junctional molecules to preserve epithelial barrier. The number of IEL markedly increased when oocyst production reached a peak. During infection, IEL increased production of gamma interferon (IFN-γ) and tumor necrosis factor alpha (TNF-α) and decreased transforming growth factor β (TGF-β) production. Addition of IFN-γ and TNF-α or supernatants obtained from cultured IEL from *E. vermiformis*-infected mice reduced transepithelial electrical resistance (TER) in a confluent CMT93 cell monolayer, a murine intestine-derived epithelial line, but antibodies against these cytokines suppressed the decline of TER. Moreover, TGF-β attenuated the damage of epithelial monolayer and changes in TER caused by IFN-γ and TNF-α. The expression of junctional molecules by EC was decreased when IEL produced a high level of IFN-γ and TNF-α and a low level of TGF-β in *E. vermiformis*-infected mice. Interestingly, IEL constantly expressed junctional molecules and a coculture of EC with IEL increased TER. These results suggest that IEL play important multifunctional roles not only in protection of the epithelium against *E. vermiformis*-induced change by cytokine production but also in direct interaction with the epithelial barrier when intra-EC junctions are down-regulated.**

Eimeria spp., are intracellular protozoan parasites (phylum: Apicomplexa) closely related to infectious pathogens of humans such as *Cryptosporidium* spp. (38). *Eimeria* spp. infect the intestinal epithelial cells (EC) of numerous animals including rodents and livestock, and *Eimeria* sp.-infected animals often show growth retardation and morbidity and mortality (4, 16). Currently, an enormous economic problem in the livestock business is caused by infection with *Eimeria* spp., leading to intestinal coccidiosis involving a bloody diarrhea, sloughing of the epithelium, and death of the host (39). Although inflammatory tissue injury has been reported to closely correlate with the oocyst output from the host (3), the involvement of immunological events with disruption of barrier function in intestinal epithelium during *Eimeria* sp. infection has remained unclear.

Eimeria vermiformis, a murine pathogen, has been widely used as a coccidial model in the laboratory to elucidate the mechanism of host protection against primary and secondary infections. T cells bearing T-cell receptor αβ (TCRαβ) (αβ T cells) are necessary for protecting the host against infection, whereas γδ T cells are important for repairing lesions as regulatory cells (31). It is assumed that the effects of T cells in protection against *E. vermiformis* are partially mediated by cytokines, such as gamma interferon (IFN-γ) and tumor necrosis factor alpha (TNF-α), because these cytokines have been detected in *E. vermiformis*-infected hosts (27). IFN-γ-deficient or -depleted mice are highly susceptible to infection (40, 41). IFN-γ is produced in *E. vermiformis*-infected hosts, especially at the site of infection. Although intestinal intraepithelial lymphocytes (IEL) reside at a basolateral site of the intestinal epithelium, no studies have examined the role of cytokine production by IEL during *E. vermiformis* infection.

The epithelial lining of the gastrointestinal tract forms a regulated, selectively permeable barrier between the luminal contents and the underlying tissue compartments by junctional molecules. The junction complex constitutes the primary barrier against the paracellular penetration of intestinal microorganisms. In particular, tight junction complexes, which are formed by occludin, a plasma membrane protein, and zonula occludens (ZO), its cytoplasmic partner protein, are linked to the actin cytoskeleton (23). Selective disturbance of tight junction complexes by microorganisms results in the rapid decrease of transepithelial electrical resistance (TER) of the EC layer, resulting in increasing paracellular permeability (20). Re-

* Corresponding author. Mailing address: Parasitic Diseases Unit, Department of Infectious Diseases, Faculty of Medicine, University of Miyazaki, Kiyotake, Miyazaki 889-1692, Japan. Phone: 81-985-85-0990. Fax: 81-985-84-3887. E-mail: INAGAKI@med.miyazaki-u.ac.jp.

cently, we demonstrated that IEL express a range of junctional molecules associated with EC (15). Both IFN-γ and TNF-α are elevated in the inflammatory mucosa, showing a contribution to the proinflammatory cascade, which may be involved in barrier disruption (24, 26). Hence, we examined cytokine production by IEL and their involvement in epithelial function to understand the contribution of IEL in maintaining an epithelial barrier during enteric infection.

MATERIALS AND METHODS

Mice. Male C57BL/6 mice were purchased at the age of 8 weeks from the Japan SLC (Hamamatsu, Japan). All mice were used between 8 and 12 weeks of age, and protocols were approved by the institutional review board for animal experiments of the University of Miyazaki.

Infection by *E. vermiformis*. *E. vermiformis* was passaged in mice, and oocysts were purified and sporulated (33). After microscopical scoring of stocks for sporulation, mice were given 100 or 500 sporulated oocysts in 100 μl of water by oral gavage. During infection, feces were collected every 3 days. Oocysts were counted on McMaster chambers after salt flotation.

Histological analysis. Intestines were fixed with 4% paraformaldehyde in phosphate-buffered saline and embedded in paraffin. The paraffin sections were stained with hematoxylin-eosin.

Cell preparation. Following *E. vermiformis* infection, mice were euthanized and both IEL and EC in the small intestine were isolated and prepared every 3 days according to a modification of previously published methods (12). In brief, after the small intestine was divided into the upper one-third (including the duodenum) and the lower two-thirds (from the jejunum to the ileum), dissected small segments of each part were incubated at 37°C for 30 min in RPMI 1640 medium (Sigma Chemical Co., Missouri) containing 10% fetal calf serum and 1 mM dithiothreitol with vigorous shaking. The tissue suspension was passaged through a nylon mesh to remove debris and centrifuged through a 25%-40%-75% discontinuous Percoll (Sigma) gradient at 600 × *g* at 20°C for 20 min. The cells collected from the interface of 40%-75% and 25%-40% were IEL and EC, respectively.

Cell culture and cytokine analysis. Whole and sorted IEL (1×10^6/ml) were added to a 96-well plate precoated with 2.5 μg anti-CD3ε monoclonal antibody (MAb) (145-2C11; BD Pharmingen) and were cultured for 48 h in RPMI 1640 supplemented with 10% fetal calf serum, 100 U/ml penicillin, and 100 U/ml streptomycin. The supernatants were collected to estimate the cytokine contents. The contents of cytokines in the culture supernatant were assayed by an enzyme-linked immunosorbent assay (ELISA) system using mouse IFN-γ, interleukin-4 (IL-4), and TNF-α (*e*-bioscience, San Diego, Calif.) and transforming growth factor β (TGF-β) (Biosource International Inc., Camarillo, Calif.). ELISA systems were used according to the manufacturer's instructions.

Analysis of mRNA expression of junctional molecules. Total RNA was extracted from isolated cells using the RNeasy Mini kit (QIAGEN, Valencia, Calif.) and primed with 20 pmol of a random primer in mixtures for reverse transcription. The synthesized cDNA was amplified by PCR using primers specific for the murine junctional molecules and β-actin cDNA sequence. The primer sets were described as previously reported for reverse transcription-PCR (RT-PCR) (15): ZO-1, sense, 5′-CAA AGC CCA CCA AGG TCA C-3′, and antisense, 5′-TCT CTT TCC GAG GCA TTA GCA-3′; occludin, sense, 5′-CAG GGC TCT TTG GAG GAA-3′, and antisense, 5′-TAC ACG ATC GTG GCA ATA AAC-3′; junctional adhesion molecule (JAM), sense, 5′-GAC CCG GAA GGA CAA TGG AGA-3′, and antisense, 5′-AGG ACA GCT GCC ACG ATG C-3′; β-catenin, sense, 5′-ACT GTT CTA CGC CAT CAC GAC-3′, and antisense, 5′-CCT CTA TGC CAC CCA CTT G-3′; E-cadherin, sense, 5′-GCA CAT ATG TAG CTC TCA TC-3′, and antisense, 5′-CCT TCA CAG TCA CAC ACA TG-3′; desmoglein 2, sense, 5′-GGA CTT TGG AAA CGG ACT TC-3′, and antisense, 5′-TCT GTA ATT CCC TTC CCA GTG-3′; connexin 26, sense, 5′-GCT CAC GGT CCT CTT CAT CT-3′, and antisense, 5′-ACC CTT CGA TAC GGA CCT TCT-3′; β-actin, sense, 5′-TGG AAT CCT GTG GCA TCC ATG AAA C-3′, and antisense, 5′-TAA AAC GCA GCT CAG TAA CAG TCC G-3′. For quantitative analysis of mRNA, the synthesized cDNA was amplified by using primers and probes specific for ZO-1 and occludin and β-actin cDNA sequence (TaqMan gene expression assays; Applied Biosystems, Foster City, Calif.) according to the manufacturer's instructions. Quantitative real-time PCR was performed by using an ABI Prism 7000 sequence detector system (Applied Biosystems, Foster City, Calif.). Results are expressed as difference (*n*-fold) from the expression of β-actin.

Western blotting analysis. Western blotting analysis was performed as previously reported (15). In brief, isolated EC and IEL were washed with cold phosphate-buffered saline and lysed in sample buffer (125 mM Tris, pH 6.8, 2% sodium dodecyl sulfate, 10% glycerol, and 2% 2-mercaptoethanol) at 95°C for 7 min, followed by sonication for 1 min. Proteins were electrophoresed and transferred to a polyvinylidene difluoride membrane. The membrane was blocked with 10% skimmed milk in Tris-buffered saline–Tween for 1 h, incubated with each Ab against junctional proteins overnight at 4°C, and then incubated with appropriate horseradish peroxidase-labeled secondary Abs (affinity-purified goat anti-rabbit, goat anti-mouse, or goat anti-rat immunoglobulin G) that were obtained from Jackson ImmunoResearch Labs Inc. (West Grove, Pa.). Bound antibodies were visualized by enhancement with chemiluminescence substrate (Pierce, Rockford, Ill.). The primary Abs against junctional molecules used in Western blotting were as follows: rabbit antioccludin (Zymed; cytoplasmic domain specific), rabbit antioccludin (Santa Cruz; extracellular/cytoplasmic domain), mouse anti-β-catenin (BD Transduction Laboratories), goat anti-JAM1 (Santa Cruz Biotechnology, Inc., Santa Cruz, Calif.), goat anti-E-cadherin (extracellular domain specific; R&D Systems Inc., Minneapolis, MN), and mouse anti-desmoglein (BD Transduction Laboratories). Mouse anti-β-actin Ab was purchased from Sigma (St. Louis, Mo.).

Fluorescence-activated cell sorting analysis. IEL were stained with fluorescein isothiocyanate-conjugated TCRγδ (GL3), phycoerythrin-conjugated TCRβ (H57-597), and allophycocyanin-conjugated CD3ε (145-2C11) MAbs as described previously (13). Flow cytometry analysis was performed on a FACScalibur flow cytometer (Becton Dickinson, Franklin Lakes, NJ). All MAbs were purchased from BD Pharmingen (San Jose, Calif.).

Measurement of TER. Functional integrity of tight junctions in cell layers established on filter inserts was assessed by measuring TER using a Millicel ERS volt-ohmmeter (Millipore Corp., Bedford, Mass.). The CMT93 cell line, a mouse intestine-derived epithelial line, was obtained from the American Type Culture Collection (CCL223). CMT93 cells were seeded on the apical chamber of a transwell by using the BD BioCoat Intestinal Epithelium Differentiation Environment (BD Biosciences, Bedford, Mass.) for 72 h in a 5% CO_2 incubator according to the manufacturer's instructions and developed a TER around 450 Ω/cm^2. After that, culture medium was removed from the apical and basolateral chamber and replaced with either fresh medium or medium containing IFN-γ (1, 10, or 100 ng/ml) (Chemicon, Temecula, Calif.), TNF-α (1, 10, or 100 ng/ml) (Peprotech EC, London, United Kingdom), or TGF-β (2.5 ng/ml) (Roche Diagnostics, Mannheim, Germany) and cultured for 48 h. To examine the effect of cytokines produced by IEL in *E. vermiformis*-infected mice on the barrier of CMT93 cells, mice were euthanized at each day after *E. vermiformis* infection and IEL were prepared. IEL were stimulated with plate-bound anti-CD3 MAb for 48 h, and the supernatant was recovered. The culture medium from the apical and basolateral chamber was removed and replaced with the supernatant. For neutralization of IFN-γ and TNF-α, anti-IFN-γ and anti-TNF-α MAbs (BioLegend, San Diego, Calif.) were added to culture wells at 10 μg/ml. The TER without a cellular monolayer was consistently less than 70 Ω/cm^2. For primary EC culture, EC were isolated as described previously (12) and 5×10^5 cells were seeded on the apical chamber of a transwell by using the BD BioCoat Intestinal Epithelium Differentiation Environment for 6 days to develop a TER around 200 Ω/cm^2. A varying number of IEL were added onto cultured EC on day 4 after the start of culture, and 2 days later, TER was measured. Values of TER are expressed as percentages of the initial resistance as follows: % of the initial resistance = [(resistance from each point) − (resistance from a blank)/(resistance from nontreated cells) − (resistance from a blank)] × 100.

Depletion of IFN-γ or TNF-α in vivo. Five hundred micrograms of anti-IFN-γ MAb (R4-6A2) (21) or 50 μg of anti-TNF-α MAb (1F3F3; Bender MedSystems Products, Vienna, Austria) or rat immunoglobulin G (Cappel, North Carolina) was administered intraperitoneally into the mice on days −1, 3, and 7 after infection.

Statistical analysis. Student's *t* test was used to determine the significant differences. A *P* value of less than 0.05 was taken as significant.

RESULTS

Preference of *E. vermiformis* for infecting the small intestine. *E. vermiformis* infects the lower part (jejunum to ileum) of the murine small intestine (46), confirmed in the present study in C57BL/6 mice with 100 oocysts (Fig. 1). Alteration of the structure, such as enlarged crypt EC, breakage at the villus tip (arrows in Fig. 1f), and mound-like villi (arrowhead in Fig. 1c),

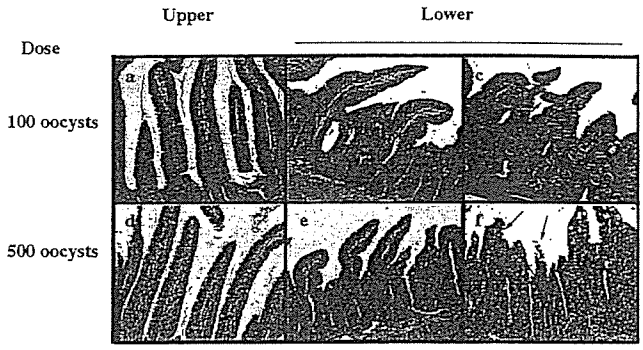

FIG. 1. Hematoxylin-and-eosin-stained transverse sections of the small intestine on day 9 p.i. Mice were given 100 or 500 oocysts of *E. vermiformis*. On day 9 p.i., the small intestine was removed and divided into parts, the upper (including duodenum [a and d]) and the lower (jejunum [b and e] and ileum [c and f]) (magnification, ×200).

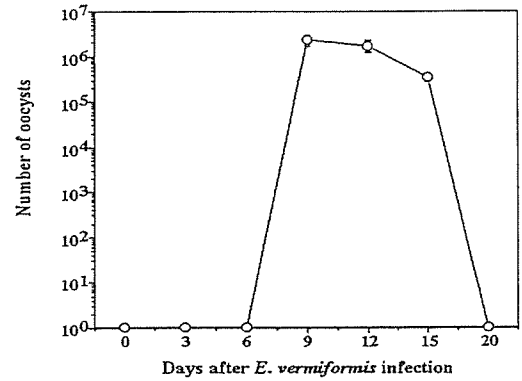

FIG. 2. Oocyst output of *E. vermiformis* in C57BL/6 mice. Mice were orally infected with 100 oocysts of *E. vermiformis*, and the oocyst output was determined every 3 days. Three mice were used in each point. Values represent the mean ± standard deviation of three individual experiments.

was observed in the lower segment of the small intestine in an *E. vermiformis* dose-dependent manner. We noted that when mice were infected with a higher dose (>1,000 oocysts) of *E. vermiformis*, some succumbed before the infection had spread throughout the jejunum (data not shown). In addition, the body weight of the mice infected with 100 oocysts was not altered. Based on these observations, we used 100 oocysts of *E. vermiformis* to infect mice in subsequent experiments. Oocyst production increased from days 6 to 9 postinfection (p.i.) with *E. vermiformis* and then gradually decreased (Fig. 2).

Changes in the kinetics of IEL subsets following *E. vermiformis* infection. While staining the tissue sections with hematoxylin and eosin, we noticed that the number of IEL in the upper one-third was much higher than that in the lower two-thirds of the small intestine in healthy mice (26/100 EC in the upper segment versus 11/100 EC in the lower segment). In addition to the regulatory function of IEL for EC (12, 18, 49), IEL have been shown to change in response to *E. vermiformis* infection (8). We confirmed these findings. The difference in the infection pattern with *E. vermiformis* between the upper and lower segments of the small intestine (46) (Fig. 1) allowed assessment of compartmentalization in the response induced by infection of the lower small intestine. Although *E. vermiformis* infection was not observed in the upper segment, the total number of IEL seen in infected mice increased temporally on day 9 p.i. and then decreased to the preinfection levels, while the number in the lower segment did not change significantly (Fig. 3A). Murine IEL comprise an approximately equal frequency of T cells bearing TCRαβ (αβ IEL) and TCRγδ (γδ IEL) (10). We also examined the changes in the population of αβ IEL and γδ IEL during *E. vermiformis* infection. As shown in Fig. 3B, a larger number of γδ IEL were present in the upper segment before infection and then decreased until day 15 p.i., whereas αβ IEL increased following infection. Both αβ and γδ IEL in the upper segment almost recovered to the preinfection level on day 20 p.i. In the lower segment, αβ IEL and γδ IEL were nearly equal in number. αβ IEL increased until day 15 p.i., whereas γδ IEL decreased. The number of γδ IEL was lower than that of αβ IEL during infection except for the early stage of infection in the upper segment (days 0 to 3 p.i.). Both αβ and γδ IEL in the lower segment of the small intestine recovered to the initial level on day 20 p.i. These results indicate that the total number of IEL increased at around a peak of oocyst production, which was due to an increase in αβ IEL rather than γδ IEL.

Production of preventive cytokines by IEL in *E. vermiformis*-infected mice. Cytokine balance is important for protection against or susceptibility to infection. IFN-γ, a typical Th1-type cytokine, has been shown to be important against primary infection with *E. vermiformis* (35, 41). *E. vermiformis* development occurs within EC; hence, IEL, which reside between EC, are well placed to influence parasite development and to maintain the integrity of the EC barrier. IEL are reported to produce both Th1 and Th2 cytokines (48); thus, it is important to determine which cytokines are produced by IEL during *E. vermiformis* infection. We examined the production of cytokines IFN-γ, IL-4 (a typical Th2-type cytokine), and TNF-α (an inflammatory cytokine) by IEL in the upper and lower segments of the gut during infection. As shown in Fig. 4, IFN-γ, IL-4, and TNF-α were increased in IEL after infection, reached a peak on days 6 to 12 p.i., and then recovered to the initial level on day 20 p.i. In contrast, TGF-β (a Th3-type and immunoregulatory cytokine) decreased and reached a minimum on days 12 to 15 p.i and recovered to the initial level on day 20 p.i. These changes in the cytokines occurred after oocyst shedding (Fig. 2). TGF-β was produced in greater quantities in the upper segment than in the lower segment of the small intestine, and large quantities of TNF-α were produced in the lower segment during infection.

Effects of cytokines produced by IEL on the epithelial barrier. We next examined whether cytokines produced by IEL directly affect the epithelial barrier function. In order to examine the functional integrity of the epithelial barrier, we measured TER in CMT93 cells, which were cultured in a transwell. The CMT93 cell layer progressively lost TER in a dose-dependent manner when the cells were cultured with IFN-γ or TNF-α (Fig. 5A). TER was further decreased when CMT93 cells were cultured in combination with IFN-γ and TNF-α (Fig. 5B). As TGF-β has been known not only to repair mucosal injury but also to preserve the integrity of the intestinal mucosa (6, 28), we examined the effect of TGF-β on TER

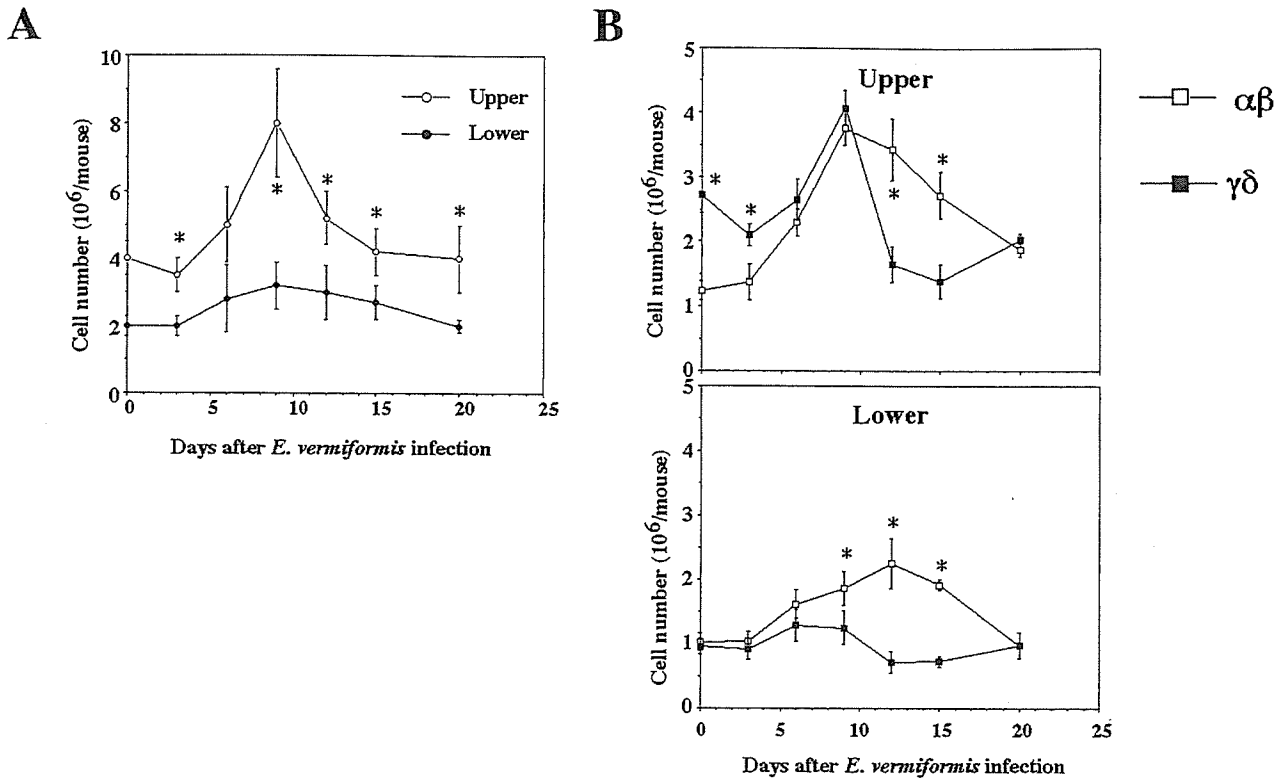

FIG. 3. Cell number of IEL following infection with *E. vermiformis*. (A) Total IEL number was counted by staining with trypan blue. (B) Population of IEL bearing TCRαβ and TCRγδ of the upper and lower parts following infection. IEL were stained with fluorescein isothiocyanate-conjugated TCRγδ MAb, PE-conjugated TCRβ MAb, and allophycocyanin-conjugated CD3ε MAb. The TCRαβ and TCRγδ expression was gated on $CD3^+$ cells. Three mice were used in each point. Values represent the mean ± standard deviation of three individual experiments in a triplicate assay. Asterisks represent statistically significant differences ($P < 0.05$).

in CMT93 cells. Although TER in CMT93 cells was decreased by the addition of TNF-α or IFN-γ alone (Fig. 5A), it was increased by the addition of TNF-α plus TGF-β or IFN-γ plus TGF-β (Fig. 5B). TER was not affected by addition of TGF-β alone. Antibodies against TNF-α or IFN-γ suppressed the decline of TER in CMT93 cells. Furthermore, when CMT93 cells were cultured with the supernatant of IEL derived from the upper or lower segment of the small intestine from noninfected mice, TER decreased to 84% or 82%, respectively (Fig. 5C). TER in CMT93 cells decreased to 68% when CMT93 cells were cultured with the supernatant obtained from IEL from the upper segment of the infected mice on day 6 p.i. In contrast, TER was more intensively reduced (54%) by exposure to the supernatant of IEL from the lower segment of the infected mice. The decreased TER in CMT93 cells was significantly reversed by the addition of anti-IFN-γ and anti-TNF-α Abs, confirming that these cytokines directly affect TER. These results indicate that the epithelial barrier could be impaired through inflammatory cytokines produced by IEL in *E. vermiformis*-infected mice.

Decreased expression of junctional molecules in EC during *E. vermiformis* infection. An established clinical manifestation of coccidiosis is a reproducible fluid loss at the peak of infection (30), suggesting involvement of the physical damage and

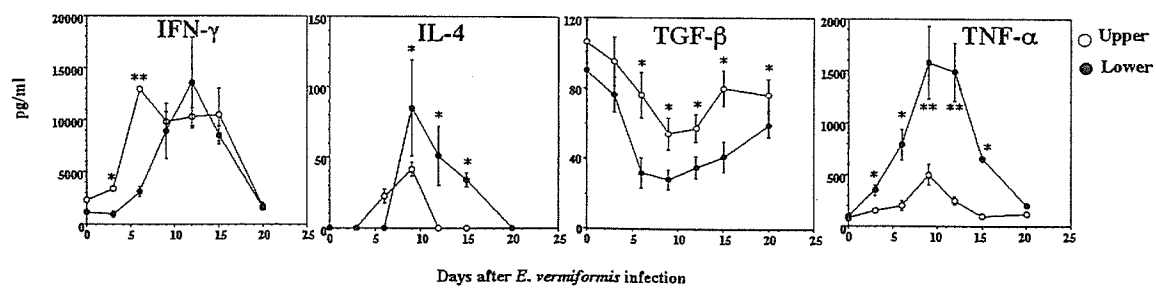

FIG. 4. Changes in cytokine production of IEL following infection with *E. vermiformis*. Freshly isolated IEL at each time point were cultured with plate-bound anti-CD3 MAb for 48 h, and the supernatants were collected to determine the concentration of each cytokine by ELISA for IFN-γ, IL-4, TNF-α, and TGF-β. Three mice were used in each point. Values represent the mean ± standard deviation of three individual experiments in a triplicate assay. Asterisks represent statistically significant differences (*, $P < 0.05$; **, $P < 0.01$).

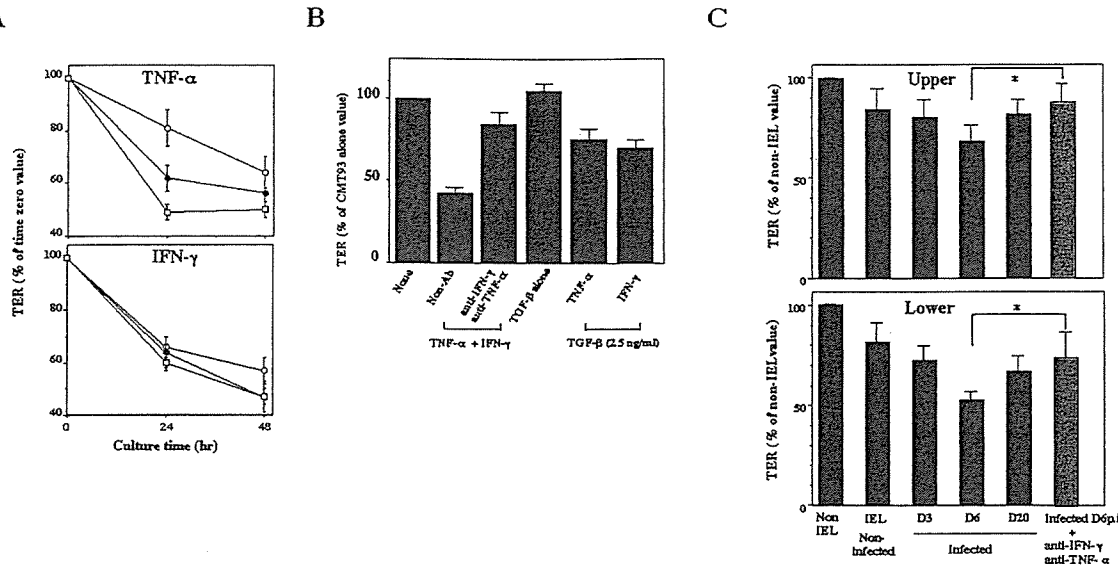

FIG. 5. Abolishment of TER in an epithelial cell line by inflammatory cytokines produced by IEL. (A) CMT93 cells were exposed to 1 (open circles), 10 (closed circles), and 100 (open squares) ng/ml of recombinant IFN-γ or TNF-α for 24 and 48 h. (B) CMT93 cells were cultured in combination with 10 ng/ml of IFN-γ and TNF-α. for 48 h. CMT93 cells were also cultured with 2.5 ng/ml of TGF-β1 and IFN-γ or TNF-α (10 ng/ml) for 48 h. (C) CMT93 cells were cultured with supernatants of IEL prepared from mice infected with *E. vermiformis* on days 3, 6, and 20 p.i. in the presence of immobilized anti-CD3 MAb. Supernatant prepared from mice infected with *E. vermiformis* on day 6 p.i. was added with 10 μg/ml of anti-IFN-γ and anti-TNF-α Abs to CMT93 cells. These cells were then incubated for 48 h at 37°C for the determination of TER. Values represent the mean ± standard deviation of three individual experiments in a triplicate assay. Asterisks represent statistically significant differences (*, $P < 0.05$).

disruption of the epithelial barrier as shown in Fig. 1. To maintain the integrity of the intestinal barrier, EC express junctional molecules such as tight junction (ZO-1, occludin, and JAM), adherens junction (β-catenin and E-cadherin), desmosome (desmoglein 2), and gap junction (connexin 26) at the apical-to-basolateral sites to prevent paracellular mutual crossing of a body fluid and of a variety of luminal contents (2, 36). In order to determine how the epithelial barrier is impaired in the *E. vermiformis*-infected mice, we examined the expression level of specific mRNA for a variety of junctional molecules in small intestinal EC. In the upper segment of the small intestine, the mRNA expression of occludin, JAM, β-catenin, and desmoglein 2 remarkably decreased on day 6 p.i. (Fig. 6A). In the lower segment, in addition to these junctional molecules, the expression of E-cadherin was also decreased. The expression of these molecules was partially recovered on day 9 p.i. and completely on day 12 p.i. in the upper segment. In contrast, the recovery of these molecules in the lower segment was delayed in comparison with that in the upper part. Since ZO-1 and occludin are crucially important for formation of TER, we

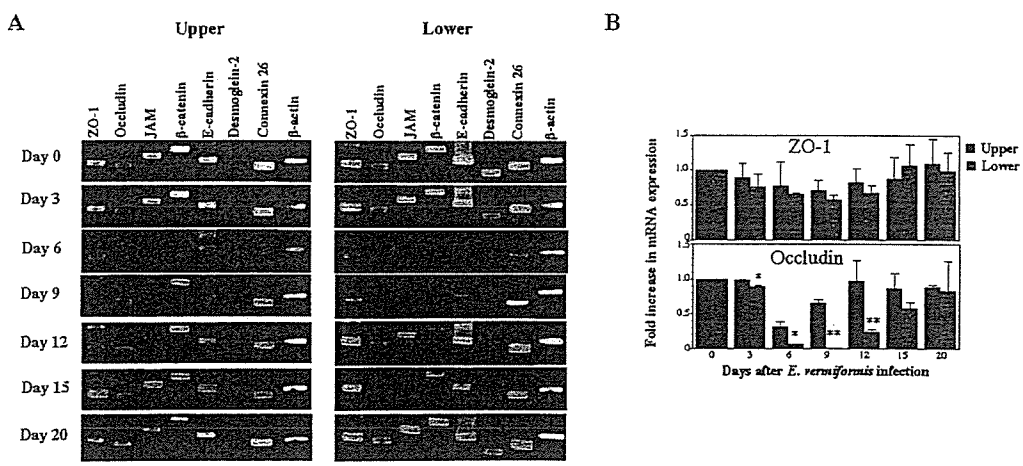

FIG. 6. Decreased mRNA expression of junctional molecules in small intestinal EC following infection with *E. vermiformis*. (A) Total RNA was prepared from EC of small intestine and amplified by RT-PCR. (B) mRNA expression of ZO-1 and occludin was analyzed quantitatively by real-time PCR. Data are presented as the ratio of each time point to day 0 in the upper and lower segment. Asterisks represent statistically significant differences between the upper and lower segments (*, $P < 0.05$; **, $P < 0.01$).

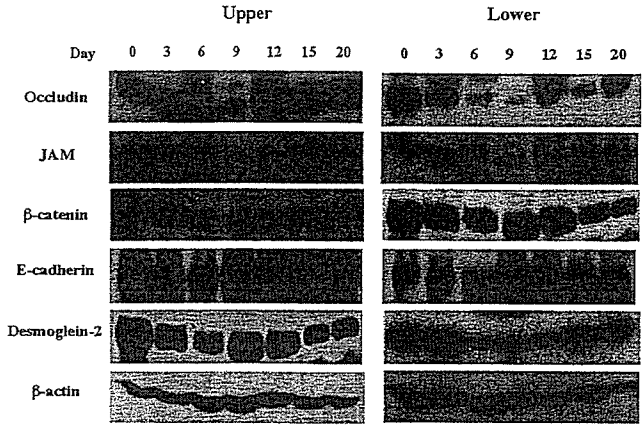

FIG. 7. Western blotting analysis for the expression of junctional molecules at the protein level in EC of small intestine. Cell lysate was prepared from small intestinal EC in mice and analyzed by Western blotting as described in Materials and Methods.

further examined these proteins' expression by real-time RT-PCR. The expression of occludin mRNA in the lower segment is less than that in the upper segment, whereas expression of ZO-1 was not altered, consistent with RT-PCR data in Fig. 6A.

We further confirmed the expression of occludin, JAM, β-catenin, E-cadherin, and desmoglein 2 in EC at the protein level (Fig. 7). In the lower segment, the expression of occludin, one of the tight junction molecules, continued to decrease from day 3 p.i. to day 9 p.i. and then recovered. The expression of JAM also decreased on days 6 and 9 p.i. The expression of β-catenin, E-cadherin, and desmoglein, which are located basolaterally in the enterocytes, was shown to decrease on day 6 p.i. and then increased until day 15 p.i. In the upper segment, although JAM and β-catenin transiently decreased, expression was rapidly recovered. These findings suggest a strong relationship between the impairment of expression of junctional molecules by EC and the severity of the infection-induced lesions.

Expression of junctional molecules in IEL during *E. vermiformis* infection and maintenance of the epithelial barrier by IEL. We recently reported that IEL constitutively express junctional molecules, similar to EC, especially occludin and E-cadherin, strongly suggesting that IEL bind to and interact with EC (15). We examined the expression of occludin and E-cadherin in IEL during infection with *E. vermiformis*. Unlike EC, occludin and E-cadherin expressed by IEL did not decrease following infection at either the mRNA or the protein level (Fig. 8A and B). These results indicate that the junctional molecules in IEL, but not in EC, are maintained during infection.

We further examined whether IEL can maintain an epithelial barrier function of EC by measuring TER of freshly iso-

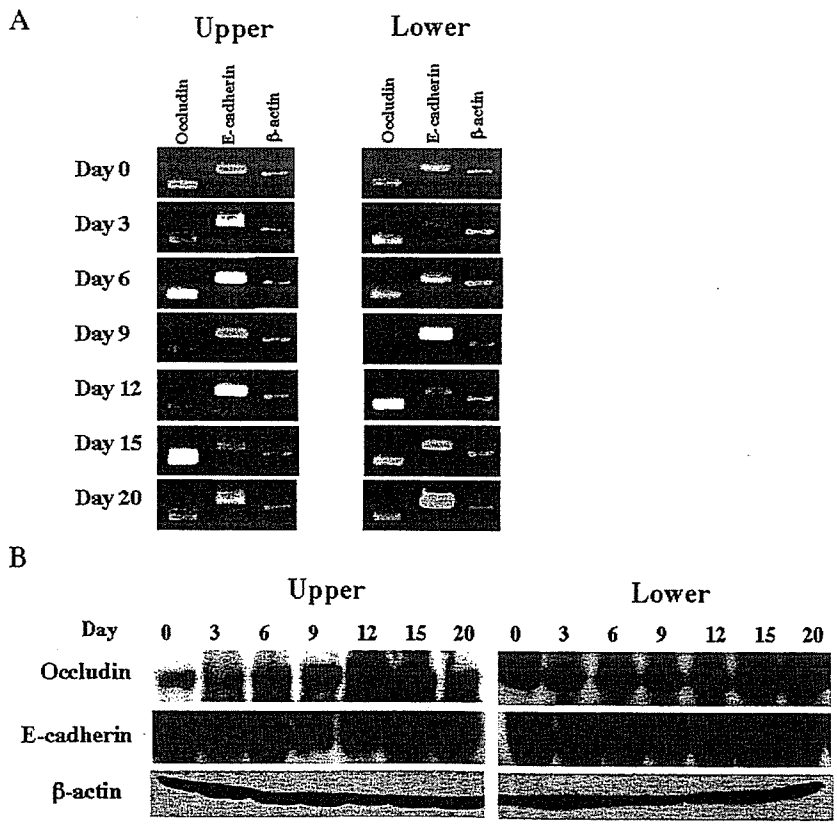

FIG. 8. Sustained mRNA expression of junctional molecules in small intestinal IEL following infection with *E. vermiformis*. After small intestine was separated into upper and lower segments, fresh IEL were obtained. (A) Total RNA was prepared from IEL in the upper and lower parts and amplified by RT-PCR. (B) Western blotting analysis for the expression of junctional molecules at protein level in IEL of small intestine. Cell lysate was prepared from small intestinal IEL in the upper and lower segments and analyzed by Western blotting.

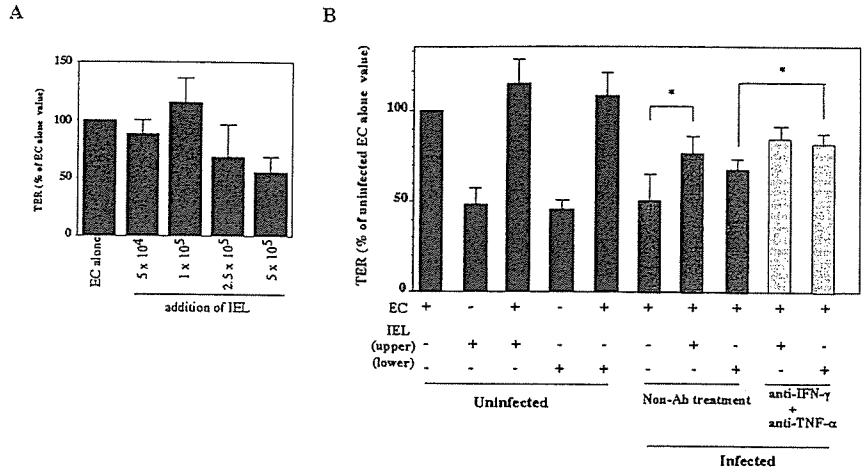

FIG. 9. Increased TER in freshly isolated EC cocultured with IEL from *E. vermiformis*-infected mice on day 6 p.i. (A) Effect of a varying number of IEL on TER of EC. On day 4 after EC were cultured, IEL were added to EC and TER was measured on day 6. Values represent the mean ± standard deviation of three individual experiments in a triplicate assay. (B) On day 4 after EC were cultured, 1×10^5 IEL were added to EC, and TER was measured with or without 10 μg/ml of anti-IFN-γ and anti-TNF-α Abs on day 6. Values represent the mean ± standard deviation of three individual experiments in a triplicate assay. Asterisks represent statistically significant differences ($P < 0.05$).

lated EC. Freshly isolated EC of the small intestine reached a maximal TER on day 6 after the start of the culture (data not shown). Titration of the number of IEL applied to EC on day 4 of culture revealed that maximum TER on day 6 was achieved with 1×10^5 IEL (Fig. 9A). As shown in Fig. 9B, TER did not change significantly when EC alone or EC plus IEL from noninfected mice were cultured. In contrast, TER markedly decreased when EC prepared from infected mice were used. Interestingly, TER of EC recovered when cocultured with IEL in the upper segment of the small intestine of infected mice but not with IEL in the lower segment. The decreased TER in EC recovered after the treatment of mice with

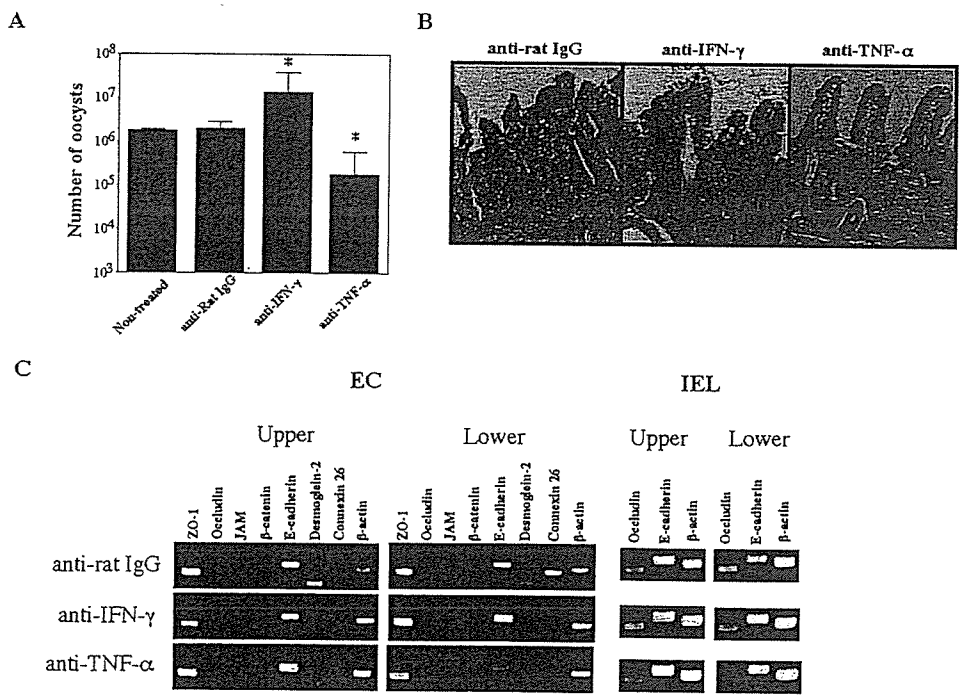

FIG. 10. Modulation of junctional molecules due to depletion of IFN-γ or TNF-α in vivo. (A) Oocyst output of *E. vermiformis* in mice treated with anti-IFN-γ Ab or anti-TNF-α Ab in vivo. Mice were orally infected with 100 oocysts of *E. vermiformis*, and the oocyst output was determined on day 9 p.i. Values represent the mean ± standard deviation of three mice in each group. Asterisks represent statistically significant differences (*, $P < 0.05$). (B) Hematoxylin-and-eosin-stained transverse sections of the small intestine on day 9 p.i. (magnification, ×200). (C) mRNA expression of junctional molecules in small intestinal EC following infection with *E. vermiformis*. Total RNA was prepared from EC of small intestine and amplified by RT-PCR. IgG, immunoglobulin G.

anti-IFN-γ and anti-TNF-α Abs confirmed that these cytokines decrease TER in EC in vivo. IEL die easily when separated and cultured in isolation (13). However, we observed that approximately 60% of IEL remained alive at 48 h in the transwell under the present experimental conditions (data not shown). Collectively, these results suggest that IEL contribute to the maintenance of an epithelial barrier in *E. vermiformis*-infected mice.

Effects of IFN-γ and TNF-α on inhibition of growth of *E. vermiformis* and in exaggeration of epithelial damage. IFN-γ and TNF-α were increased in *E. vermiformis*-infected mice (Fig. 4), and these cytokines diminished epithelial barrier function (Fig. 5). We examined the role of IFN-γ and TNF-α in modulation of intestinal epithelial barrier against *E. vermiformis* infection by using IFN-γ- or TNF-α-depleted mice. As previously reported (41), anti-IFN-γ Ab-treated mice produced approximately 10-fold-more oocysts than control Ab-treated mice on day 9 p.i. (Fig. 10A). By contrast, anti-TNF-α Ab-treated mice showed markedly lower levels of oocyst output. Histological analysis revealed that anti-IFN-γ Ab-treated mice exhibited more severe intestinal damage than control immunoglobulin G or anti-TNF-α Ab-treated mice did in the lower segment (Fig. 10B). We further examined expression of junctional molecules by EC in anti-IFN-γ or -TNF-α Ab-treated mice. Treatment with anti-IFN-γ Ab or anti-TNF-α Ab alone failed to recover expression of junctional molecules, which are suppressed by *Eimeria* infection (Fig. 10C), compared with the level of the expression in noninfected mice (Fig. 6A, day 0 panel). These results suggest that IFN-γ is an important cytokine in protective immunity against *Eimeria* infection and that TNF-α may exacerbate infection. Epithelial damage was affected by the level of infection and also influenced by the activity of cytokines in vivo.

DISCUSSION

The disruption of the epithelial barrier has been reported in intestinal diseases including those induced by infection. IEL are located to play protective roles against infection, repair of a damaged mucosal barrier, and maintenance of the barrier function in the intestine. The present study focused upon IEL as a defender of the host against the consequences of *E. vermiformis* infection, and we found that IEL play an important role in sustaining the barrier function via maintaining the expression of junctional molecules as well as by producing cytokines against *E. vermiformis* infection. These data strongly suggest that IEL function both as constituent cells of the physical epithelial barrier during infection and in killing pathogens in local intracellular infection.

It has long been considered that IEL serve a critical role in the mucosal immune system by performing a variety of regulatory functions, including cytokine production, cytotoxic activity, and induction of apoptosis in EC (11, 14, 44, 48). *E. vermiformis* infects the lower segment of the small intestine in mice (46), and infection-induced inflammation and damage of tissue were restricted to this segment (Fig. 1). We found that the total number of IEL in the upper segment is relatively larger than that in the lower segment even before infection and increases further during *E. vermiformis* infection (Fig. 3A). Overall the IEL in the murine small intestine contain approximately equal populations bearing TCRαβ and TCRγδ (10); however, the results of these studies indicated rationalization of the IEL populations with greater numbers of γδ IEL in the upper part of the small intestine than in more distal regions (Fig. 3). We have reported that γδ T-cell-deficient ($C\delta^{-/-}$) mice are susceptible to trinitrobenzene sulfonic acid-induced colitis and show a fragile small intestine (12), suggesting that the residence of fewer γδ IEL in the lower part of the small intestine might cause fragility of the intestinal epithelium. Interestingly, these data might support the possibility that IEL function to prevent the spread of infection or damage to the upper segment because the number of IEL, especially αβ IEL in the upper segment, is higher from day 6 to day 9 p.i. (Fig. 3), and this alteration occurs concurrently with oocyst production (Fig. 1). Our data support the previous report that in adult mice, $CD4^+$ αβ T cells play the role of effector cells against primary infection of *E. vermiformis*, while γδ T cells play the role of regulatory cells (31). Moreover, the dynamics of IEL in noninfected regions of the small intestine reveal a level of coordination within the gut T-cell responses more extensive than that previously reported in any system. The effects of this coordination may be an important proactive response to protect uninfected regions of the gut from the potential of an infection spreading within the small intestine.

A transmission electrical microscopy study revealed that the sporozoites of *Eimeria* spp. actively invaded intestinal EC, which resulted in the disruption of internal cellular organization and extensive tissue damage, including disrupted microvilli (5). Interestingly, sporozoites likely moved from EC to EC at lateral sites because a junction structure, such as the tight junction, was not disturbed at the apical site, whereas that at the lateral or basolateral site was. In this study, decreased expression of occludin and JAM recovered from day 12 to day 15 p.i.; in contrast, E-cadherin and desmoglein 2 decreased from day 3 to day 6 p.i. (Fig. 6 and 7), suggesting that, during the schizogony stage, sporocysts and merozoites might move among adjacent cells, causing the destruction of the junction structure at the lateral site. Furthermore, it is possible that many EC are easily broken and damaged when oocysts break out of the host EC. Our study provides evidence that the expression of junctional proteins at the apical site, such as occludin and JAM, was reduced. We have recently demonstrated that IEL constitutively express junctional molecules, such as occludin and E-cadherin, and that the expression of these proteins is higher in γδ IEL than in αβ IEL (15). We showed in this study that IEL, unlike EC, constantly express E-cadherin and occludin during all periods of *E. vermiformis* infection (Fig. 8). It would be interesting to determine why and how the sporozoites of *E. vermiformis* prefer to move within restricted sites of the epithelium. For example, *Clostridium perfringens* enterotoxin binds to claudin 3 and 4, the molecules in the tight junction (9, 43). The surface of *Listeria monocytogenes* interacts with the extradomain of E-cadherin (19, 25, 37). These reports suggest that junctional molecules may be receptors for invading microorganisms. Therefore, it is likely that *E. vermiformis* could also bind to certain junctional molecules to move between EC. Further information is needed to prove these hypotheses.

Although eimerian infection is controlled by IFN-γ and $CD4^+$ T cells restricted to major histocompatibility complex

class II (41), it is noteworthy that IL-4 mRNA was up-regulated during infection. The production of antigen-specific IL-5 was also noted with ex vivo assays (32), and it is clear that a Th1/Th2 mixed cytokine profile is induced by infection. Nonetheless, unlike IFN-γ, IL-4 deficiency does not alter the level of oocyst output (41) and the role of Th2-type cytokines in the biology of eimerian infections is unknown, although it might be speculated that these could reduce the level of Th1-type cytokines in the gut, performing a regulatory role to reduce immune-mediated damage.

The disruption of the EC barrier might be also mediated through cytokines that are produced by IEL, a hypothesis supported by the findings of the present study. During the eimerian infection, IEL transiently produced high amounts of IFN-γ and TNF-α associated with a decrease in production of TGF-β, suggesting an interaction between production of these cytokines by IEL and that by EC. IFN-γ is well established as an important anti-*Eimeria* molecule in vitro (34) and in vivo (35, 41), as is the anti-inflammatory role for TGF-β (17, 29). Hence, our model is that the production of a high amount of IFN-γ is involved in parasite killing, whereas the infection is controlled and then resolution of the intestinal lesions is coordinated by IEL and production of TGF-β. These cytokines are known to be involved in the alteration of junctional molecules. The expression of junctional molecules on the IEL would also help to provide a structural framework for EC recovery and promote close juxtaposition between IEL and the damaged/recovering EC.

IFN-γ down-regulates the occludin promoter of the human intestinal cell line HT-29/B6 and modulates junction integrity (24, 26). On the other hand, it is well known that TGF-β regulates multiple physiological functions in various tissues, including intestinal EC, and that γδ IEL can produce TGF-β (7). Recently, we reported that the transfer of γδ IEL to $C\delta^{-/-}$ mice ameliorated trinitrobenzene sulfonic acid-induced colitis mediated by TGF-β (12). TGF-β was shown to enhance the barrier function of T84 intestinal epithelial monolayers and to promote intestinal epithelial restitution (6, 28). In our data, the IFN-γ-mediated loss of TER in CMT93 cells was normalized by addition of TGF-β (Fig. 4B). These results strongly support the hypothesis that TGF-β is necessary for the maintenance of intestinal epithelial integrity. Indeed, TNF-α induces damage in the lower segment of the small intestine after infection and was produced in the greatest amounts from IEL in the infected segment of the small intestine (Fig. 4). Taken together, our results suggest that IEL positively produce Th1-type cytokines, such as IFN-γ, to protect the host against *E. vermiformis*. Moreover, IEL might function to prevent the excessive disruption of the epithelial layer through IEL-derived cytokines by maintaining the expression of junctional molecules and production of TGF-β. It would also be interesting to determine why junctional molecules expressed by EC are remarkably down-regulated, while those in IEL are maintained during *E. vermiformis* infection (Fig. 7 and 8). This might be explained by the fact that intestinal EC possess a TNF receptor (TNFR) as well as an IFN-γ receptor (1). TNF-α has been shown to down-regulate occludin but not ZO-1 in astrocytes (47). This down-regulation of occludin was entirely mediated by TNFR1. TNFR consists of TNFR1 and TNFR2 (22, 42). TNF-α binds to both receptors; however, TNFR1 is mainly expressed on nonlymphocytes, such as EC and fibroblasts (45). Further studies will be needed to elucidate what kinds of signals from the cytokine receptor are linked to the gene expression of junctional molecules in EC and IEL and how this occurs.

ACKNOWLEDGMENTS

This work was supported by grants-in-aid for scientific research (C) from the Japan Society for the Promotion of Science (17590373), the Takeda Science Foundation (K.I.-O.), and the 21st Century COE program (University of Miyazaki) from the Ministry of Education, Culture, Sports, Science and Technology of Japan. A.L.S. received support from BBSRC and DEFRA of the United Kingdom.

We thank Goro Matsuzaki (University of the Ryukyus, Japan) for carefully reading and providing critical comments. We also thank Noriko Kanemaru for technical assistance and Joko Shigenobu and Ayumi Tanaka for their steadfast support.

REFERENCES

1. **Baumgart, D. C., W. A. Olivier, T. Reya, D. Peritt, J. L. Rombeau, and S. R. Carding.** 1998. Mechanisms of intestinal epithelial cell injury and colitis in interleukin 2 (IL2)-deficient mice. Cell. Immunol. **187**:52–66.
2. **Berkes, J., V. K. Viswanathan, S. D. Savkovic, and G. Hecht.** 2003. Intestinal epithelial responses to enteric pathogens: effects on the tight junction barrier, ion transport, and inflammation. Gut **52**:439–451.
3. **Blagburn, B. L., and K. S. Todd, Jr.** 1984. Pathological changes and immunity associated with experimental *Eimeria vermiformis* infections in *Mus musculus*. J. Protozool. **31**:556–561.
4. **Chapman, H. D.** 2001. Use of anticoccidial drugs in broiler chickens in the USA: analysis for the years 1995 to 1999. Poult. Sci. **80**:572–580.
5. **Chobotar, B., H. D. Danforth, and R. Entzeroth.** 1993. Ultrastructural observations of host-cell invasion by sporozoites of *Eimeria papillata* in vivo. Parasitol. Res. **79**:15–23.
6. **Dignass, A. U., and D. K. Podolsky.** 1993. Cytokine modulation of intestinal epithelial cell restitution: central role of transforming growth factor beta. Gastroenterology **105**:1323–1332.
7. **Ehrhardt, R. O., W. Strober, and G. R. Harriman.** 1992. Effect of transforming growth factor (TGF)-beta 1 on IgA isotype expression. TGF-beta 1 induces a small increase in $sIgA^+$ B cells regardless of the method of B cell activation. J. Immunol. **148**:3830–3836.
8. **Findly, R. C., S. J. Roberts, and A. C. Hayday.** 1993. Dynamic response of murine gut intraepithelial T cells after infection by the coccidian parasite *Eimeria*. Eur. J. Immunol. **23**:2557–2564.
9. **Fujita, K., J. Katahira, Y. Horiguchi, N. Sonoda, M. Furuse, and S. Tsukita.** 2000. *Clostridium perfringens* enterotoxin binds to the second extracellular loop of claudin-3, a tight junction integral membrane protein. FEBS Lett. **476**:258–261.
10. **Guy-Grand, D., N. Cerf-Bensussan, B. Malissen, M. Malassis-Seris, C. Briottet, and P. Vassalli.** 1991. Two gut intraepithelial $CD8^+$ lymphocyte populations with different T cell receptors: a role for the gut epithelium in T cell differentiation. J. Exp. Med. **173**:471–481.
11. **Guy-Grand, D., M. Malassis-Seris, C. Briottet, and P. Vassalli.** 1991. Cytotoxic differentiation of mouse gut thymodependent and independent intraepithelial T lymphocytes is induced locally. Correlation between functional assays, presence of perforin and granzyme transcripts, and cytoplasmic granules. J. Exp. Med. **173**:1549–1552.
12. **Inagaki-Ohara, K., T. Chinen, G. Matsuzaki, A. Sasaki, Y. Sakamoto, K. Hiromatsu, F. Nakamura-Uchiyama, Y. Nawa, and A. Yoshimura.** 2004. Mucosal T cells bearing TCR-γδ play a protective role in intestinal inflammation. J. Immunol. **173**:1390–1398.
13. **Inagaki-Ohara, K., H. Nishimura, A. Mitani, and Y. Yoshikai.** 1997. Interleukin-15 preferentially promotes the growth of intestinal intraepithelial lymphocytes bearing gamma delta T cell receptor in mice. Eur. J. Immunol. **27**:2885–2891.
14. **Inagaki-Ohara, K., H. Nishimura, T. Sakai, D. H. Lynch, and Y. Yoshikai.** 1997. Potential for involvement of Fas antigen/Fas ligand interaction in apoptosis of epithelial cells by intraepithelial lymphocytes in murine small intestine. Lab. Investig. **77**:421–429.
15. **Inagaki-Ohara, K., A. Sawaguchi, T. Suganuma, G. Matsuzaki, and Y. Nawa.** 2005. Intraepithelial lymphocytes express junctional molecules in murine small intestine. Biochem. Biophys. Res. Commun. **331**:977–983.
16. **Jenkins, M. C.** 2001. Advances and prospects for subunit vaccines against protozoa of veterinary importance. Vet. Parasitol. **101**:291–310.
17. **Kitani, A., I. J. Fuss, K. Nakamura, O. M. Schwartz, T. Usui, and W. Strober.** 2000. Treatment of experimental (trinitrobenzene sulfonic acid) colitis by intranasal administration of transforming growth factor (TGF)-beta1 plasmid: TGF-beta1-mediated suppression of T helper cell type 1 response occurs by interleukin (IL)-10 induction and IL-12 receptor beta2 chain downregulation. J. Exp. Med. **192**:41–52.

18. **Komano, H., Y. Fujiura, M. Kawaguchi, S. Matsumoto, Y. Hashimoto, S. Obana, P. Mombaerts, S. Tonegawa, H. Yamamoto, S. Itohara, et al.** 1995. Homeostatic regulation of intestinal epithelia by intraepithelial gamma delta T cells. Proc. Natl. Acad. Sci. USA **92**:6147–6151.
19. **Lecuit, M., S. Dramsi, C. Gottardi, M. Fedor-Chaiken, B. Gumbiner, and P. Cossart.** 1999. A single amino acid in E-cadherin responsible for host specificity towards the human pathogen *Listeria monocytogenes*. EMBO J. **18**: 3956–3963.
20. **Li, E., W. F. Stenson, C. Kunz-Jenkins, P. E. Swanson, R. Duncan, and S. L. Stanley, Jr.** 1994. *Entamoeba histolytica* interactions with polarized human intestinal Caco-2 epithelial cells. Infect. Immun. **62**:5112–5119.
21. **Li, Y., K. Ishii, H. Hisaeda, S. Hamano, M. Zhang, K. Nakanishi, T. Yoshimoto, H. Hemmi, K. Takeda, S. Akira, Y. Iwakura, and K. Himeno.** 2004. IL-18 gene therapy develops Th1-type immune responses in *Leishmania major*-infected BALB/c mice: is the effect mediated by the CpG signaling TLR9? Gene Ther. **11**:941–948.
22. **Loetscher, H., Y. C. Pan, H. W. Lahm, R. Gentz, M. Brockhaus, H. Tabuchi, and W. Lesslauer.** 1990. Molecular cloning and expression of the human 55 kd tumor necrosis factor receptor. Cell **61**:351–359.
23. **Madara, J. L.** 1998. Regulation of the movement of solutes across tight junctions. Annu. Rev. Physiol. **60**:143–159.
24. **Mankertz, J., S. Tavalali, H. Schmitz, A. Mankertz, E. O. Riecken, M. Fromm, and J. D. Schulzke.** 2000. Expression from the human occludin promoter is affected by tumor necrosis factor alpha and interferon gamma. J. Cell Sci. **113**:2085–2090.
25. **Mengaud, J., H. Ohayon, P. Gounon, R. M. Mege, and P. Cossart.** 1996. E-cadherin is the receptor for internalin, a surface protein required for entry of *L. monocytogenes* into epithelial cells. Cell **84**:923–932.
26. **Oshima, T., F. S. Laroux, L. L. Coe, Z. Morise, S. Kawachi, P. Bauer, M. B. Grisham, R. D. Specian, P. Carter, S. Jennings, D. N. Granger, T. Joh, and J. S. Alexander.** 2001. Interferon-gamma and interleukin-10 reciprocally regulate endothelial junction integrity and barrier function. Microvasc. Res. **61**:130–143.
27. **Ovington, K. S., L. M. Alleva, and E. A. Kerr.** 1995. Cytokines and immunological control of *Eimeria* spp. Int. J. Parasitol. **25**:1331–1351.
28. **Planchon, S. M., C. A. Martins, R. L. Guerrant, and J. K. Roche.** 1994. Regulation of intestinal epithelial barrier function by TGF-beta 1. Evidence for its role in abrogating the effect of a T cell cytokine. J. Immunol. **153**: 5730–5739.
29. **Powrie, F., J. Carlino, M. W. Leach, S. Mauze, and R. L. Coffman.** 1996. A critical role for transforming growth factor-beta but not interleukin 4 in the suppression of T helper type 1-mediated colitis by CD45RB(low) $CD4^+$ T cells. J. Exp. Med. **183**:2669–2674.
30. **Ramsburg, E., R. Tigelaar, J. Craft, and A. Hayday.** 2003. Age-dependent requirement for γδ T cells in the primary but not secondary protective immune response against an intestinal parasite. J. Exp. Med. **198**:1403–1414.
31. **Roberts, S. J., A. L. Smith, A. B. West, L. Wen, R. C. Findly, M. J. Owen, and A. C. Hayday.** 1996. T-cell alpha beta + and gamma delta + deficient mice display abnormal but distinct phenotypes toward a natural, widespread infection of the intestinal epithelium. Proc. Natl. Acad. Sci. USA **93**:11774–11779.
32. **Rose, M. E., P. Hesketh, R. K. Grencis, and A. J. Bancroft.** 2000. Vaccination against coccidiosis: host strain-dependent evocation of protective and suppressive subsets of murine lymphocytes. Parasite Immunol. **22**:161–172.
33. **Rose, M. E., D. G. Owen, and P. Hesketh.** 1984. Susceptibility to coccidiosis: effect of strain of mouse on reproduction of *Eimeria vermiformis*. Parasitology **88**:45–54.
34. **Rose, M. E., A. L. Smith, and D. Wakelin.** 1991. Gamma interferon-mediated inhibition of *Eimeria vermiformis* growth in cultured fibroblasts and epithelial cells. Infect. Immun. **59**:580–586.
35. **Rose, M. E., D. Wakelin, and P. Hesketh.** 1989. Gamma interferon controls *Eimeria vermiformis* primary infection in BALB/c mice. Infect. Immun. **57**: 1599–1603.
36. **Schneeberger, E. E., and R. D. Lynch.** 2004. The tight junction: a multifunctional complex. Am. J. Physiol. Cell Physiol. **286**:C1213–C1228.
37. **Schubert, W. D., C. Urbanke, T. Ziehm, V. Beier, M. P. Machner, E. Domann, J. Wehland, T. Chakraborty, and D. W. Heinz.** 2002. Structure of internalin, a major invasion protein of *Listeria monocytogenes*, in complex with its human receptor E-cadherin. Cell **111**:825–836.
38. **Shields, J. M., and B. H. Olson.** 2003. *Cyclospora cayetanensis*: a review of an emerging parasitic coccidian. Int. J. Parasitol. **33**:371–391.
39. **Shirley, M. W.** 1992. Research on avian coccidia: an update. Br. Vet. J. **148**:479–499.
40. **Smith, A. L., and A. C. Hayday.** 2000. An alphabeta T-cell-independent immunoprotective response towards gut coccidia is supported by gamma-delta cells. Immunology **101**:325–332.
41. **Smith, A. L., and A. C. Hayday.** 2000. Genetic dissection of primary and secondary responses to a widespread natural pathogen of the gut, *Eimeria vermiformis*. Infect. Immun. **68**:6273–6280.
42. **Smith, C. A., T. Davis, D. Anderson, L. Solam, M. P. Beckmann, R. Jerzy, S. K. Dower, D. Cosman, and R. G. Goodwin.** 1990. A receptor for tumor necrosis factor defines an unusual family of cellular and viral proteins. Science **248**:1019–1023.
43. **Sonoda, N., M. Furuse, H. Sasaki, S. Yonemura, J. Katahira, Y. Horiguchi, and S. Tsukita.** 1999. *Clostridium perfringens* enterotoxin fragment removes specific claudins from tight junction strands: evidence for direct involvement of claudins in tight junction barrier. J. Cell Biol. **147**:195–204.
44. **Taguchi, T., W. K. Aicher, K. Fujihashi, M. Yamamoto, J. R. McGhee, J. A. Bluestone, and H. Kiyono.** 1991. Novel function for intestinal intraepithelial lymphocytes. Murine $CD3^+$, gamma/delta TCR^+ T cells produce IFN-gamma and IL-5. J. Immunol. **147**:3736–3744.
45. **Tartaglia, L. A., and D. V. Goeddel.** 1992. Two TNF receptors. Immunol. Today **13**:151–153.
46. **Todd, K. S., Jr., and D. L. Lepp.** 1971. The life cycle of *Eimeria vermiformis* Ernst, Chobotar and Hammond, 1971 in the mouse *Mus musculus*. J. Protozool. **18**:332–337.
47. **Wachtel, M., M. F. Bolliger, H. Ishihara, K. Frei, H. Bluethmann, and S. M. Gloor.** 2001. Down-regulation of occludin expression in astrocytes by tumour necrosis factor (TNF) is mediated via TNF type-1 receptor and nuclear factor-κB activation. J. Neurochem. **78**:155–162.
48. **Yamamoto, M., K. Fujihashi, M. Amano, J. R. McGhee, K. W. Beagley, and H. Kiyono.** 1994. Cytokine synthesis and apoptosis by intestinal intraepithelial lymphocytes: signaling of high density alpha beta T cell $receptor^+$ and gamma delta T cell $receptor^+$ T cells via T cell receptor-CD3 complex results in interferon-gamma and interleukin-5 production, while low density T cells undergo DNA fragmentation. Eur. J. Immunol. **24**:1301–1306.
49. **Yamamoto, M., K. Fujihashi, K. Kawabata, J. R. McGhee, and H. Kiyono.** 1998. A mucosal intranet: intestinal epithelial cells down-regulate intraepithelial, but not peripheral, T lymphocytes. J. Immunol. **160**:2188–2196.

Editor: J. L. Flynn

Available online at www.sciencedirect.com
SCIENCE DIRECT®
ELSEVIER
Veterinary Parasitology 140 (2006) 158–161
veterinary parasitology
www.elsevier.com/locate/vetpar

Short communication

Evaluation of enzyme-linked immunosorbent assays with recombinant antigens for the serodiagnosis of equine *Babesia* infections

Xiaohong Huang [a], Xuenan Xuan [a], Naoaki Yokoyama [a], Yoshinari Katayama [b], Toru Anzai [b], Ikuo Igarashi [a,*]

[a] *National Research Center for Protozoan Diseases, Obihiro University of Agriculture and Veterinary Medicine, Inada-cho, Obihiro, Hokkaido 0808555, Japan*
[b] *Microbiology Division, Epizootic Research Institute of Japan Racing Association, Kokubunji-machi, Shimotsuga-gun, Tochigi 329-0412, Japan*

Received 5 December 2005; received in revised form 1 March 2006; accepted 10 March 2006

Abstract

Two enzyme-linked immunosorbent assays (ELISA) with recombinant protein as antigens were evaluated by comparison with the indirect fluorescent antibody tests (IFAT) for the detection of specific antibodies to *Babesia caballi* and *Babesia equi*, respectively in 380 sera from experimentally infected, uninfected, and field horses. The high concordances of 92.4% (351/380) and 98.2% (373/380) between ELISA and IFAT for *B. caballi* and *B. equi*, respectively suggest that ELISA, especially for *B. equi* infection, could be alternative to the corresponding IFAT for serodiagnoses of equine piroplasmosis, although some improvements are required in ELISA for *B. caballi*.

Keywords: *B. caballi*; *B. equi*; Bc48; EMA-2t; ELISA

Equine piroplasmosis, caused by two tick-borne haemoprotozoan *Babesia caballi* and *Babesia equi*, is generally characterized by fever, anemia, jaundice, edema, and even death of the infected horses (Holbrook, 1969; de Waal, 2000), which result in great economic losses in the horse industry in many tropical and subtropical areas. Up to date, Japan is considered as free of the disease. However, the detection of carrier status in imported animals is necessary to prevent the introduction of the infected horses to Japan due to the increasing number of horses imported from endemic areas and the existence of tick vectors *Dermacentor reticulus* and *Rhipicephalus sanguineus* (Yoshihara, 1997). Recently, two enzyme-linked immunosorbent assays (ELISAs) were reported for *B. caballi* (Ikadai et al., 1999, 2000) and *B. equi* (Knowles et al., 1997; Huang et al., 2003). In the present study, we report the evaluation of the ELISAs by comparison with indirect fluorescent

* Corresponding author. Tel.: +81 155 49 5641; fax: +81 155 49 5643.
E-mail address: igarcpmi@obihiro.ac.jp (I. Igarashi).

0304-4017/$ – see front matter © 2006 Elsevier B.V. All rights reserved.
doi:10.1016/j.vetpar.2006.03.013

Table 1
Comparison of BcELISA and BcIFAT in the detection of anti-*B. caballi*-specific antibody

Test	Positive no. (%)					Overall concordance no. (%)
	Pre-infection (**18**)	*B. caballi* Infected (**65**)	*B. equi* Infected (**67**)	Field sera		
				Domestic (**195**)	Imported (**35**)	
BcIFAT	1 (0.06)	55 (84.6)	1 (1.5)	8 (3.8)	4 (11.4)	351 (92.4)
BcELISA	0 (0)	50 (76.9)	5 (7.5)	15 (7.0)	4 (11.4)	

The bold numbers are the sample numbers examined in each group. The total number examined was 380.

antibody tests (IFATs) for the detection antibodies to *B. caballi* and *B. equi* using serum samples collected from experimentally infected, uninfected or field horses.

For *B. caballi* infection, the recombinant 48 kDa merozoite rhoptry protein with glutathione *S*-transferase tag (GST-Bc48) (Kappmeyer et al., 1999; Ikadai et al., 1999, 2000) was used as an antigen with minor modification of reducing the expression temperature from 37 to 25 °C to increase the yield of soluble protein during antigen preparation. For *B. equi* infection, the recombinant truncated *B. equi* merozoite antigen-2 with GST tag (GST-EMA-2t) was used and prepared as described previously (Knowles et al., 1997; Huang et al., 2003). GST was used as control antigen in both ELISAs. Each test was designated as BcELISA and BeELISA for the detection of specific antibody to *B. caballi* and *B. equi*, respectively.

ELISAs were performed as described previously (Huang et al., 2003). According to the preliminary tests, the optimal concentration of GST-Bc48 and GST-EMA-2t (1 and 5 μg/ml, respectively), the optimal dilutions of sera (1:100) and horseradish peroxidase-conjugated goat anti-horse immunoglobulin G (ICN Biochemicals, USA) (1:2000) were used. The optical density (OD) at 415 nm was read by using an MTP-120 ELISA reader (Corona Electric, Japan). The final OD of each sample was the difference of the average reading from duplicate test wells with that from duplicate GST control wells. The cut-off value was calculated from the mean absorbance with three times of standard deviation ($\bar{X} + 3$S.D.) of 15 known negative horse sera detected. It was 0.2 in BcELISA and 0.07 in BeELISA. A sample was considered to be positive if the calculated absorbance was equal to or greater than the cut-off value.

IFATs were performed as described previously (Madden and Holbrook, 1968; Morzaria et al., 1977). The tests were designated as BcIFAT and BeIFAT for the detection of specific antibodies to *B. caballi* and *B. equi*, respectively. A sample was considered to be positive when its titer reached 1:80.

Three hundred and eighty horse serum samples were used. Out of these samples, 195 were from healthy racing horses in Japan, 18 from horses pre-infection, 65 from horses infected experimentally with *B. caballi* 8–38 days post-infection (dpi), 67 from horses infected experimentally with *B. equi* 6–38 dpi, and 35 from imported horses that were suspected to be *Babesia*-infected, respectively.

Out of 65 serum samples from horses experimentally infected with *B. caballi*, 55 and 50 samples were BcIFAT-postive and BcELISA-postive, respectively (Table 1). Comparison between BcELISA and BcIFAT indicated that out of 55 BcIFAT-positive sera, 6 serum samples before 14 dpi were BcELISA-negative (date not shown), and these results suggest that BcELISA was less sensitive than BcIFAT in the detection of earlier stage of infection, at which the specific antibody titer in sera might be very low. The loss of sensitivity might be the consequences of higher sera dilution in BcELISA than that in BcIFAT. It might be also due to that native Bc48 did not expose to the host as early as surface antigens did during infection, therefore, the appearance of the specific antibody to native Bc48 occurs later. In *B. equi*-infected group, samples of 7.5% (5/67) were BcELISA-positive, which was higher than 1.5% (1/67) of BcIFAT-positive. The loss of specificity in BcELISA might be resulted from the contamination of antigen.

Out of 67 serum samples from horses experimentally infected with *B. equi*, 62 and 63 samples were BeIFAT-postive and BeELISA-postive, respectively (Table 2). Only one of 62 BeIFAT-positive samples was BeELISA-negative, in reverse, two of five BeIFAT-negative sera were BeELISA positive (data not shown). The results revealed that BeELISA was

Table 2
Comparison of BeELISA and BeIFAT in the detection of anti-*B. equi*-specific antibody

Test	Positive no. (%)					Overall concordance no. (%)
	Pre-infection (**18**)	*B. caballi* Infected (**65**)	*B. equi* Infected (**67**)	Field sera		
				Domestic (**195**)	Imported (**35**)	
BeIFAT	1 (0.06)	0 (0)	62 (92.5)	1 (0.005)	25 (71.4)	373 (98.2)
BeELISA	0 (0)	0 (0)	63 (94.0)	0 (0)	27 (77.1)	

The bold numbers are the sample numbers examined in each group. The total sample number was 380.

more sensitive than BeIFAT. In addition, all 18 sera from horses pre-infection were BeELISA-negative, suggesting BeELISA was more specific than BeIFAT by which one of 18 sera pre-infection was positive.

The BcELISA and BeELISA positive rates were 7.0% and 0 in domestic horse, and 11.4% and 77.1% in imported horse sera. Finally, the high concordances of 92.4% (351/380) and 98.2% (373/380) were obtained between IFAT and ELISA in *B. caballi* and *B. equi* infections, especially that between BeELISA and BeIFAT (Tables 1 and 2).

Complement fixation test (CFT) and IFAT are usually used as the official tests for equine piroplasmosis in many countries. IFAT is more sensitive than CFT, and the sera remain positive by IFAT longer than CFT (Tenter and Friedhoff, 1986). Compared with ELISA, however, IFAT is time consuming and requires large amounts of parasites. Moreover, the estimation of the intensity of fluorescence is subjective and requires the participation of experts, which has hindered the standardization and comparability of the results. In the ELISAs, the recombinant antigens expressed by *Escherichia coli* were used. *E. coli* is easier to store, culture, extract, and purify than the native parasites used in IFAT. The high efficacy of the expression of GST-rEMA2t and GST-Bc48 in *E. coli* made BeELISA and BcELISA more economical and feasible for large-scale production for commercial use, which will result in the standardization of the serodiagnoses of *B. equi* and *B. caballi* infections in horses. In conclusion, our results indicate that BeELISA are comparable and superior to BeIFAT and that it could be applicable as an alternative test for the serodiagnosis of equine piroplasmosis. On the other hand, although BcELISA need some improvements, its overall concordance to BeIFAT and the listed advantages of ELISA suggested that BcELISA also may be acceptable as an alternative test to BcIFAT for the serodiagnosis of *B. caballi* infection.

Acknowledgements

This study was supported by a grant from The 21st Century COE Program (A-1), Ministry of Education, Culture, Sports, Science, and Technology, Japan, and Grants-in-Aid for Scientific Research from the Japan Society for the Promotion of Science.

References

de Waal, D.T., 2000. Global importance of piroplasmosis. J. Protozool. Res. 10, 106–127.

Holbrook, A.A., 1969. Biology of equine piroplasmosis. Am. J. Vet. Med. Assoc. 155, 453–454.

Huang, X., Xuan, X., Yokoyama, N., Xu, L., Suzuki, H., Sugimoto, C., Nagasawa, H., Fujisaki, K., Igarashi, I., 2003. High-level expression and purification of a truncated merozoite antigen-2 of *Babesia equi* in *Escherichia coli* and its potential in immunodiagnosis. J. Clin. Microbiol. 41, 1147–1151.

Ikadai, H., Xuan, X., Igarashi, I., Tanaka, S., Kanemaru, T., Nagasawa, H., Fujisaki, K., Suzuki, N., Mikami, T., 1999. Cloning and expression of a 48-kilodalton *Babesia caballi* merozoite rhoptry protein and potential use of the recombinant antigen in an enzyme-linked immunosorbent assay. J. Clin. Microbiol. 37, 3475–3480.

Ikadai, H., Osorio, C.R., Xuan, X., Igarashi, I., Nagasawa, H., Fujisaki, K., Suzuki, N., Mikami, T., 2000. Detection of *Babesia caballi* infection by enzyme-linked immunosorbent assay using recombinant 48-kDa merozoite rhoptry protein. Int. J. Parasitol. 30, 633–635.

Kappmeyer, L.S., Perryman, L.E., Hines, S.A., Baszler, T.V., Katz, J.B., Hennager, S.G., Knowles, D.P., 1999. Detection of equine antibodies to *Babesia caballi* by recombinant *B. caballi* rhoptry-associated protein 1 in a competitive-inhibition enzyme-linked immunosorbent assay. J. Clin. Microbiol. 37, 2285–2290.